Energy Economy through the Use of Synthetic Oils in the Engine, Transmission and Two Rear Axles of a Road Transport Vehicle

CA1
DTC 800
89
E52

Date Due

APR AVR	8 1990		

BRODART, INC Cat. No. 23 233 Printed in U.S.A.

CA1
DTC800-
89
E52

MM

425791

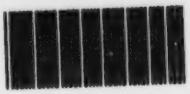

41.D

TP 8140E

Energy Economy through the Use of Synthetic Oils in the Engine, Transmission and Two Rear Axles of a Road Transport Vehicle

Prepared for the

Transportation Development
Centre
Transport Canada

by

Forest Engineering Researach Institute
of Canada

Library and Information Centre / Centre de Documentation (ASTA)
RECEIVED - REÇU LE
NOV 28 1989
Transport Canada / Transports Canada

NOVEMBER 1986

DDN 422288

90-01734/

TP 8140E

Energy Economy through the Use of Synthetic Oils in the Engine, Transmission and Two Rear Axles of a Road Transport Vehicle

by

D.A. Ljubic

Forest Engineering Research Institute of Canada

November 1986

NOTICE

The opinions and views expressed in this report are the author's and do not necessarily reflect those of the Transportation Development Centre of Transport Canada.

Ce rapport est disponible en français sous le titre "Économies d'énergie résultant de l'utilisation des huiles synthétiques dans le moteur, la transmission et les deux essieux arrière d'un véhicule routier", TP 8140F.

Research Team

D.A. LJUBIC, technical director of project

J. MICHAELSEN, assistant and researcher

Y. PROVENCHER, test researcher

R. LEVESQUE, computer analyst

J. LABRIE, instrument expert

D. MACGREGOR, technician

Transport Canada / Transports Canada
Development / Développement

REPORT DOCUMENTATION FORM

1. Transport Canada Report No.	2. TDC Project No.	3. Recipient's Catalogue No.
TP 8140E	6593-94	

4. Title and Subtitle	5. Report Date
Energy Economy through the Use of Synthetic Oils in the Engine, Transmission and Two Rear Axles of a Road Transport Vehicle	November 1986
	6. Performing Organization Report No.

7. Author(s)	8. Transport Canada File No.
D.A. LJUBIC	D-1465-470

9. Performing Organization Name and Address	10. DSS File No.
Forest Engineering Research Institute of Canada (FERIC) 143, Place Frontenac Pointe Claire (Québec) H9R 4Z7	11. DSS or Transport Canada Contract No.

12. Sponsoring Agency Name and Address	13. Type of Report and Period Covered
Transportation Development Centre (TDC) 200, Dorchester Blvd West, suite 601 Montréal (Québec) H2Z 1X4	14. Sponsoring Agency Code

15. Supplementary Notes	16. TDC Project Officer
Co-sponsored by the Energy R&D Program of Energy, Mines and Resources Canada	L. Sabounghi

17. Abstract

This report describes a study to investigate and demonstrate the reduction in energy consumption obtained through the use of synthetic oils in the engine, transmission and two rear axles of a road transport vehicle. Comparisons were made for controlled conditions during oil temperature stabilization, at constant speeds, during acceleration and under actual operating conditions. In addition, new methods of analysis were developed and verified for on-road evaluation of the energy balance of a moving vehicle.

18. Key Words	19. Distribution Statement
Engine, transmission, rear axles, synthetic oils, lubricants, vehicles, energy, fuel conservation.	Limited number of copies available from Transportation Development Centre.

20. Security Classification (of this report)	21. Security Classification (of this page)	22. No. of Pages	23. Price
Unclassified	Unclassified	74	

TDC/CDT 79-005
Rev 86

Canada

Transports Canada / Transport Canada

Développement / Development

FORMULE DOCUMENTAIRE DU RAPPORT

1. N° du rapport Transports Canada	2. N° de l'étude — CDT	3. N° de catalogue du destinataire
TP 8140F	6593-94	

4. Titre et sous-titre	5. Date du rapport
Économies d'énergie en utilisant des huiles synthétiques dans le moteur, transmission et les deux essieux arrière d'un véhicule routier.	Novembre 1986
	6. N° du rapport de l'organisme exécutant

7. Auteur(s)	8. N° de dossier Transports Canada
D.A. LJUBIC	D-1465-470

9. Nom et adresse de l'organisme exécutant	10. N° de dossier — ASC
Institut Canadien de Recherches en Génie Forestier (FERIC) 143, Place Frontenac Pointe Claire (Québec) H9R 4Z7	11. N° de contrat — ASC ou Transports Canada

12. Nom et adresse de l'organisme parrain	13. Genre de rapport et période visée
Centre de développement des transports (CDT) 200, boul. Dorchester Ouest, suite 601 Montréal (Québec) H2Z 1X4	14. Code de l'organisme parrain

15. Remarques additionnelles	16. Agent de projet — CDT
Co-parrainé par le Programme R&D énergétiques de Énergie, mines et ressources Canada	L. Sabounghi

17. Résumé

La présente étude avait pour but principal d'examiner et démontrer la réduction de la consommation d'énergie résultant de l'utilisation des huiles synthétiques dans le moteur, la transmission et les deux essieux arrière d'un véhicule routier. Les comparaisons sont données pour les conditions contrôlées en période de stabilisation des températures des huiles, en vitesse constantes, en accélération et en service réel. En outre des nouvelles méthodes d'évaluation d'équilibre énergétique directement sur la route ont été développées et vérifiées.

18. Mots-clés	19. Diffusion
Moteur, transmission, essieux arrière, huiles synthétiques, lubrifiants, véhicules, énergie, conservation de l'énergie.	Le Centre de développement des transports dispose d'un nombre limité d'exemplaires.

20. Classification de sécurité (de ce rapport)	21. Classification de sécurité (de cette page)	22. Nombre de pages	23. Prix
Non classifiée	Non classifiée	74	

ACKNOWLEDGMENTS

This study was carried out with the cooperation of FERIC researchers Jan Michaelsen, Yves Provencher, Gilles Pesant and René Levesque, technicians D. MacGregor, S. Riffou, J. Labrie, K. Hadley and Luc Desrochers and all those who are not cited here. The author is grateful to these individuals for their invaluable assistance.

The author also wishes to thank L. Sabounghi of Transport Canada's Transportation Development Centre for his assistance.

He also expresses his gratitude to the personnel of Transport Canada's Motor Vehicle Test Centre for their generous cooperation, with particular thanks to Y. Bourdon.

Dr. D. Brière, director of the Eastern Division, and Gordon Franklin, transportation research group leader and Mr. G.P. Chinn also aided in carrying out this study.

Also noteworthy was the active participation of DOMEX High-Tech Lubricants Ltd., which supplied the test oils, the truck and other assistance.

Lastly, the author is grateful to James Maclaren Industries Inc. for aid and assistance during testing at Mont-Laurier.

SUMMARY

This study was conducted by the Forest Engineering Research Institute of Canada (FERIC) for Domex High-Tech Lubricants Ltd. at the request of the Transportation Development Centre of Transport Canada. Its primary aim was to

> investigate and demonstrate the reduction in energy consumption obtained through the use of synthetic oils in the engine, transmission and two rear axles of a road transport vehicle.

The test program was reviewed by the Transportation Development Centre, Domex High-Tech Lubricants, the oil suppliers and the Forest Engineering Research Institute of Canada. The preliminary proposal called for use of the SAE comparative evaluation method involving two vehicles (one containing a synthetic oil and the other a mineral oil) and two drivers. After a given testing time, the drivers were to switch vehicles.

After examining the request, FERIC proposed a new method whereby all the factors involved could be corrected to reduce all energy consumption to the same basis. A single vehicle and driver would be used, given that the method takes account of the full range of external and internal influences. Using that approach, all temperatures affecting energy consumption were recorded, and testing was not begun until those temperatures had completely stabilized. If, in spite of all precautions, variations in temperatures were still observed (owing to changes in atmospheric conditions from one test to another), established principles were used to reduce all the results to the same basis.

To eliminate the effect of driver performance, the tests were conducted at constant speeds of 20, 40, 60, 80 and 90 km/h. To cancel the effects of wind and vertical gradients, the vehicle was driven around the track five times in both directions. The same transmission gear ratio was used throughout for the two types of test oils (15W40 and 80W90 were the mineral or "reference" oils, 5W30 and 75W90 the synthetic oils) in order to reduce consumptions to the same basis in terms of torque and the number of revolutions of the power transmission system (power train); the aim being to derive highly accurate comparisons of power demand and energy consumption. All testing at mean speeds was conducted with the oil temperatures completely stabilized in the engine, transmission and two rear axles (Fig. 15 to 19).

Tests were conducted to explore the oil temperature stabilization times and the impact of intermediate temperatures on power demand and energy consumption. Starting at very low temperatures, the vehicle was driven at an average speed of 83 km/h and continued around the track until the temperatures had completely stabilized. During stabilization the torque behind the transmission and the fuel consumption were logged. This allowed us to monitor the rise in temperatures and the corresponding drop in torque and fuel consumption (Fig. 2 to 5).

At stabilized temperatures, we ran the vehicle through stop-accelerate tests using both of the test oils, shifting through all the gears and varying the pressure on the accelerator. Those tests were repeated 5 times in either direction on the straight portion of the test track (Fig. 1), after which averages were calculated from the logged data. Torque and fuel consumption were recorded during those tests (Fig. 20 to 24).

Lastly, the two oils were tested under actual operating conditions by driving the vehicle in both directions around a road network in the Mont-Laurier area. Those tests were intended to confirm the results obtained under controlled conditions.

Two types of results were obtained:

a) determination of the forces of resistance to power train rotation owing to oil churning, and separate determination of the resistive forces owing to friction with applied torque;
b) determination of energy savings through the use of the synthetic oils, as compared to the reference oils, in the drivetrain of the truck.

As regards the determination and separation of the forces of power train resistance, we obtained results concerning:

- resistances owing to oil churning for the transmission and each individual rear axle as a function of oil temperatures and road speed, for the two test oils [see Fig. 6 to 9 and the corresponding formula (18) in the appendix];
- friction resistances owing to the application of torque as a function of road speed (see Fig. 15 and the corresponding theory in paragraph 1.3.2.5 of the appendix);
- power train efficiency as a function of road speed [see Fig. 17 and formula (22)].

With regards to the determination of energy savings through the use of the synthetic oils, as compared to the reference oils, in the drivetrain of the truck, the results were as follows:

- 1.4% reduction in fuel consumption owing to oil churning with the synthetic oils as compared to average consumption (truck at no load and under load) at 80 km/h on the road (Fig. 12);
- 19.8% reduction in truck fuel consumption with synthetic oils for the first 20 minutes of operation (engine not stabilized), 12.5% reduction from the start of testing to the end and 8.5% difference from the moment the engine temperatures are stabilized (20 min after the start) and the end of testing.
- average 6.5% reduction in fuel consumption during constant-speed testing (20, 40, 60, 80 and 90 km/h) with the synthetic oils. Of this, power train losses account for 62% of the total loss and engine losses for 38% (see Fig. 18 and 19 and the calculation of loss distribution in the text);

- reduction in fuel consumption upon acceleration testing amounting to
  - 7% with accelerator at 60% of maximum depression, and
  - 10% with accelerator at 80% of maximum depression,

  relative to the aforesaid vehicle consumption (Fig. 20, 21 and 24);
- 6% reduction in fuel consumption upon testing under actual operating conditions in the Mont-Laurier area, relative to the aforesaid average consumption (see page 30).

ANALYSIS

The oil temperature stabilization tests confirmed that the operating temperatures of the transmission and drive axle oils on transport units in much of Canada are much lower than the ideal temperatures for which the oils have been traditionally designed. Because of loading, unloading and other delays, most of the travel time during the winter is likely to be with oil temperatures not exceeding 45°C. Therefore, energy saving benefits are to be expected with oils having lower or flatter viscosity versus temperature curves in the -10°C to 100°C temperature range. However, it is very important that reduced oil churning energy losses not be obtained at the expense of inferior lubricating qualities. Thus, a superior lubricating oil must reduce the oil churning energy losses and if possible also friction losses. In such a case the oil is bringing considerable advantages to the user.

The tests confirmed that the polyalphaolefin base synthetic oils (5W30 for the engine and 75W90 for the driveline) reduced both the oil churning losses and the friction coefficients in the driveline of both the loaded and non-loaded logging truck as compared with the reference mineral oils (15W40 for the engine and 80W90 for the driveline). Under normal eastern Canadian winter conditions, the synthetic oils were calculated to provide a saving of about 6.5% of the fuel consumption for a logging truck round trip (half non-loaded and half loaded). This savings range was confirmed by a normal-duty road test in the Mont-Laurier area of Québec where fuel savings averaged 6%.

Reduced oil churning energy losses, especially at the low start-up temperatures mean that less stress must be absorbed by the moving driveline components. This, in turn, means less fatiguing of the metal parts and the probability of increasing their useful life.

A reduced friction factor should result in a reduced wear rate of the contact surfaces of the driveline's moving parts. This, also, should result in improved component life.

CONCLUSIONS

Compared to the reference mineral oils, the polyalphaolefin base synthetic oils used in this test have been shown to reduce the energy losses in a truck driveline (and, hence, fuel consumption) and can also be expected to have a beneficial effect on driveline component life. This must <u>not</u> be construed as a blanket endorsement of synthetic or semi-synthetic lubricating oils which have other formulations and which may or

may not have the 5W30 and 75W90 classifications. Each formulation must be proven by careful experimental or field tests.

While it has been theorized that the reduced oil churning energy losses and reduced friction coefficient experienced with the tested synthetic oils should improve the life of driveline components, controlled tests and component life analysis will be necessary to confirm that this is so or that the component life improvement is of a magnitude to be economically significant. A test program to measure the rate of metallic contamination of the lubricating oils for oils having different friction coefficients could provide useful information to metallurgists and the formulators of lubricating oils. Such knowledge should, ultimately, lead to improved truck performance and lower transport costs.

TABLE OF CONTENTS

1. INTRODUCTION 1

2. TEST EQUIPMENT, METHODOLOGY AND PROGRAM 2
   2.1 Test Equipment 2
   2.2 Test Methodology and Program 3

3. BRIEF DESCRIPTION OF MINERAL OILS AND SYNTHETIC OILS 5

4. THEORETICAL CONSIDERATIONS ON LUBRICATION AND HEAT EXCHANGE IN MOTOR VEHICLE DRIVETRAINS 6
   4.1 Introduction 6
   4.2 General Discussion on Lubrication 7
   4.3 Heat Exchange between Oils and Environment 9

5. TEST RESULTS 11
   5.1 Determination of Oil Churning Losses through the Power Train 11
   5.2 Determination of Losses through Tire Rolling and Air Resistance 16
   5.3 Analysis of Heat Exchange between Oils and Environment during Temperature Stabilization Testing at Average Speed of 83 km/h, with Comparison of Two Test Oils 19
   5.4 Analysis of Energy Balance on Blainville Track at Constant Road Speeds (20, 40, 60, 80 and 90 km/h) for Two Test Oils 21
   5.5 Comparison of Fuel Consumption with Two Test Oils at Different Constant Speeds 25
   5.6 Comparison of Fuel Consumption during Acceleration Testing on Blainville Track 27
   5.7 Comparison of Fuel Consumption for Two Test Oils in Normal Road Duty (Mont-Laurier, Ferme-Neuve, Lac des Écorces, Mont-Laurier) 30
   5.8 Analysis of Results 30

      5.8.1 Oil Churning Losses through Power Train 30
      5.8.2 Stabilization Tests 31
      5.8.3 Constant-Speed Road Tests 32
      5.8.4 Acceleration Testing 33
      5.8.5 Normal-Duty Testing 33

Table of Contents (cont'd)

6. CONCLUSION 34

APPENDIX 35

1. DETERMINATION OF POWER LOSSES OF A TRANSPORT VEHICLE ON THE ROAD 35
   1.1 Foreword 35
   1.2 General Description of Vehicle Energy Balance 35
   1.3 Methods of Determining Energy Balance Components for Truck-Trailer Combination 43

      1.3.1 Determination of Force F_{TDR} between Traction Wheels and Ground 43
      1.3.2 Determination of Force F_{SP} of Power Train Rotating Resistance owing to Oil Churning and Friction, N 45

         1.3.2.1 Analysis of Force F_{BH} 46
         1.3.2.2 Analysis of Moment of Inertia J 48
         1.3.2.3 Determination of Moment J_R 48
         1.3.2.4 Determination of Moment J_{SP} 50
         1.3.2.5 Analysis of Resistive Force F_{FC} owing to Applied Torque 51

      1.3.3 Analysis of Combined Forces of Air and Tire Rolling Resistance (without applied torque) 53

         1.3.3.1 Integration of Equation (56) 54
         1.3.3.2 FERIC Method (by derivation of speed-time curve) 59

2. HEAT EXCHANGE BETWEEN ENVIRONMENT, REAR AXLES AND TRANSMISSION OF A TRUCK 61

3. PROPERTIES OF TEST OILS 65

   3.1 Engine Oils 65
   3.2 Power Train Oils 65

DEFINITION OF SYMBOLS 66

REFERENCES 74

LIST OF FIGURES

Figure 1	Track at Transport Canada's Motor Vehicle Test Centre at Blainville (Québec)	3
Figure 2	Fuel consumption and torque behind transmission measured during stabilization testing on the test track	8
Figure 3	Stabilization test for engine, transmission and rear axle oil temperatures and fuel temperature	9
Figure 4	Stabilization test for engine, transmission and rear axle oil temperatures and fuel temperature	9
Figure 5	Stabilization test for engine, transmission and rear axle oil temperatures and fuel temperature	10
Figure 6	Initial force of resistance owing to oil churning in the transmission and two rear axles as a function of oil temperature--reference oil	12
Figure 7	Initial force of resistance owing to oil churning in the transmission and two rear axles as a function of oil temperature--synthetic oil	12
Figure 8	Coefficient "a" for the reference oil as a function of oil temperature	13
Figure 9	Coefficient "a" for the synthetic oil as a function of oil temperature	13
Figure 10	Oil churning resistances in the transmission and two rear axles as a function of oil temperature	15
Figure 11	Characteristic curves for Cummins 261 kW (350 hp) engine	15
Figure 12	Fuel consumption through oil churning in the transmission and two rear axles as a function of oil temperature	16
Figure 13	Diagram of distance, speed and acceleration as a function of time (free-wheeling deceleration)	17
Figure 14	Total forces of resistance for a truck-trailer combination obtained by free-wheeling deceleration as a function of speed	18

Figure 15 Energy balance on Blainville track obtained by constant speed testing 23

Figure 16 Total energy balance expressed in engine fuel consumption at different speeds 24

Figure 17 Power train ratings η_{SP} at different speeds 25

Figure 18 Comparison of total fuel consumption for two test oils as a function of speed 26

Figure 19 Comparison of fuel consumption for the two test oils as a function of speed 26

Figure 20 Comparison of fuel consumptions measured in acceleration on the track as a function of road speed 27

Figure 21 Comparison of fuel consumptions measured in acceleration on the track as a function of transmission ratio 28

Figure 22 Comparison of fuel consumption for the two test oils in acceleration as a function of transmission ratio 29

Figure 23 Comparison of fuel consumption for the two test oils in acceleration as a function of transmission ratio 29

Figure 24 Comparison of differences in fuel consumption for the two test oils in acceleration as a function of transmission ratio 30

Figure 25 Torque as determined by road speed measured during acceleration testing 32

Figure 26 Energy balance of forces acting on a transport vehicle 36

Figure 27 Speed-time diagram obtained by power train deceleration from speed v'_r to zero 46

Figure 28 Diagram of wheel rotation on a decline 52

Figure 29 Diagram representing the interpretation of free-wheeling test results 57

Figure 30 Speed-time diagram obtained by direct measurement 59

Figure 31 Diagram of translational acceleration as a function of road speed 60

1. INTRODUCTION

In late 1985, the Transportation Development Centre of Transport Canada commissioned Domex High-Tech Lubricants Ltd. to investigate and demonstrate the reduction in energy consumption resulting from the use of synthetic oils in the engine, transmission and two rear axles of a road transport vehicle. One provision of the contract called for entrusting the technical analysis to the Forest Engineering Research Institute of Canada, under the technical direction of D.A. Ljubic, senior road transport researcher.

The study was to be conducted on the test track at Transport Canada's Motor Vehicle Test Centre at Blainville (Québec).

The study commenced in November 1985 and entailed fitting a truck with a complete data logging system and making that system operational.

The test program was discussed by the Test Centre's scientific authority, DOMEX experts, the suppliers of the test oils and FERIC. The detailed program was drawn up by D.A. Ljubic. It included a number of new ideas on the evaluation of the differences regarding on-road energy balance and fuel consumption and was to serve in particular to evaluate the differences in fuel consumption in the engine and power train through the use of the mineral ("reference") oils and the synthetic oils (refer to the appendix for the properties of these oils).

The logging and analysis of the data were fully computerized, thereby minimizing human error. The impact of driver performance was also minimized.

Testing was completed in late April 1986, the data analysis and drafting of the original report in late November 1986.

2. TEST EQUIPMENT, METHODOLOGY AND PROGRAM

2.1 Test Equipment

The main purpose of this study was to make optimum comparisons of energy consumption with mineral ("reference") oils and synthetic oils used in the engine and the power train of a road truck. The truck and trailers remained unchanged throughout testing.

The following truck-trailer combination was used for off-load testing:

- Truck - FORD, LTL9000, 5.31 m wheelbase; Rockwell forward axle, 5,455 kg capacity; Rockwell SQHP rear axle, 18,182 kg capacity; 3.73 real axle ratio; Michelin 11.00X22.5 MS+4 tires in the rear and XZA in the front; Cummins NTC-350 engine (261 kW at 2100 rpm, maximum torque 1593 N•m at 1300 rpm).
- Trailer - van type, 4.25 m high (at roof), 2.44 wide and 13.72 m long, fitted with two axles with Michelin 11.00X20 XZA tires.
- Total mass - 16,000 kg.

The following tractor-trailer combination was used for on-load testing:

- Same truck;
- Trailer - forest type 4.10 m high, 2.44 m wide and 14.63 m long, fitted with 3 axles and Toyo 11RX24.5 tubeless tires.
- Total mass of loaded vehicle 46,820 kg.

These two combinations remained unchanged throughout comparison testing of the two test oils.

The truck was fitted with highly sophisticated measuring instruments connected to a data logging system that recorded pertinent variables on the moving truck at the rate of 10 and 30 times per second. This was achieved by using one of the latest systems, capable of recording on 128 channels with a maximum scanning capability of 20,000 data items per second and a storage capability of 66 MBytes.

FERIC used 24 sensors on 29 channels for this study.

Among the variables recorded were fuel consumption, torque behind the transmission, accelerator depression, front wheel steering angles, pressure before and behind the supercharging turbine, distance, time, wind velocity and direction and all temperatures necessary to correct all the tests to the same operating conditions. Other factors which can be derived from these data include road speed, power, braking, and mode of speed change.

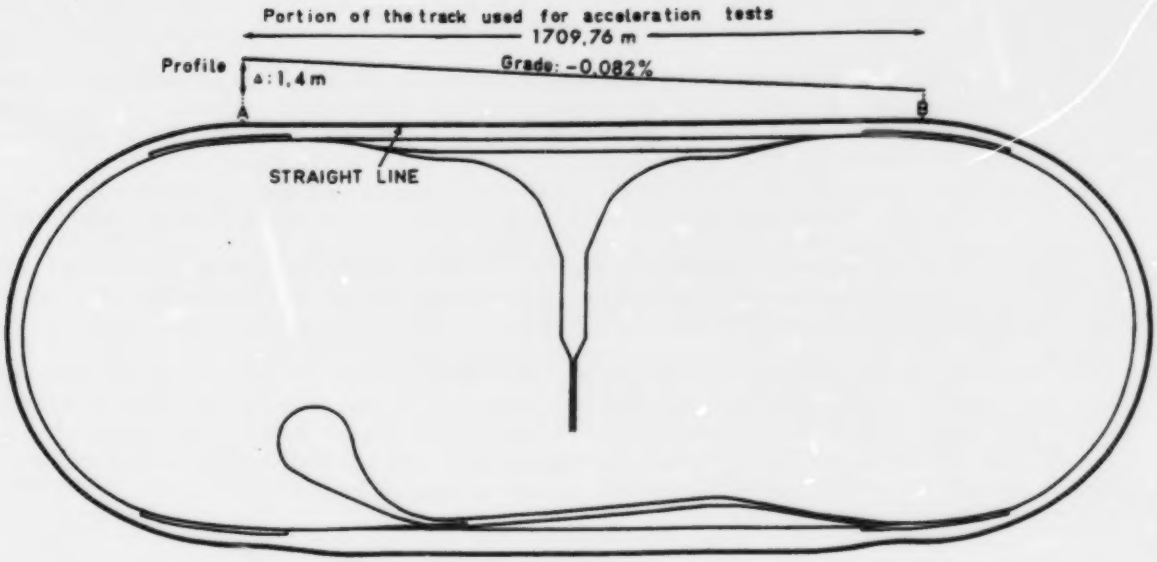

Figure 1 Track at Transport Canada's Motor Vehicle Test Centre at Blainville (Québec)

2.2 Test Methodology and Program

The method of comparison proposed by the Society of Automotive Engineers calls for two road rigs, each containing a different oil and driven by a different driver on a test track of known characteristics. Testing extends over a fairly long period of time and the rigs follow each other at a reasonable distance. After a time, the drivers change vehicles and the test cycle is repeated. See SAE standard J1264 for further details.

To streamline this procedure, making it shorter, less costly and more accurate, FERIC developed a test program requiring a single vehicle and driver.

The basic idea behind this program is the possibility of minimizing the effects of driving technique, atmospheric conditions and the thermal state of the truck's drivetrain.

The two oils were tested on the federal government's test track at Blainville (see Fig. 1), using one truck and two different trailers (one on-load and the other off-load). The program proceeded as follows:

- After leaving the truck overnight in the cold, we began driving around the track at a mean speed of about 80 km/h. The initial temperatures of the oils and fuel in the engine, transmission and two rear axles being very low (see Fig. 3 and 4), we recorded at the rate of 10 times per second the torque behind the transmission, the fuel consumption and all temperatures until their complete stabilization.

The same tests were conducted for reference oils 15W40 in the engine and 80W90 in the power train and for synthetic oils 5W30 (engine) and 75W90 (power train) (the properties of these oils are provided in the appendix).

The consumptions and torques were also obtained for different combinations of oils by virtually eliminating the effect of driver performance (constant speed). The effect of wind velocity and direction on fuel consumption was minimized given that the truck was driven around an oval track.

- Constant-speed tests were then conducted at 20, 40, 60, 80 and 90 km/h. With each of the above oils, the truck was driven around the track at the indicated speeds 5 times in each direction (about 70 km). The average consumptions and torques at each speed were thus established, again by eliminating the effects of driver performance and wind.

- Acceleration tests were then performed. With the truck at standstill, we started up and shifted through all the gears, first pressing the accelerator to the floor and then to 60% and 80% of maximum depression. Each acceleration was repeated 5 times in each direction in a straight line (see Fig. 1).

- The tests outlined below were conducted to determine the distribution of power train losses owing to oil churning and losses owing to friction with applied torque.

  a) Free-wheeling deceleration tests were run with the truck raised off the ground, with the two oils and for each separate component (transmission, forward-rear axle and rear-rear axle), starting at the lowest temperatures and continuing to maximum temperatures (determination of losses through oil churning).

  b) On-road free-wheeling deceleration tests were run in a straight line, 15 times in either direction, to cancel the effect of wind (determination of rolling and air resistance in order to calculate these parameters during analysis of the energy balance at constant speeds and in acceleration).

- Lastly, tests were conducted with the two oils under actual operating conditions (75 km circuit) 3 times around the track in both directions.

Having logged all the temperatures, we were able to make the necessary corrections to reduce them all to the same basis.

Our findings, e.g., at constant speed, in acceleration and in deceleration, were intended to quantify the differences in fuel consumption under various conditions and to study the energy balance. The results of those analyses were intended to break down power train losses into losses owing to oil churning and losses owing to friction (see theoretical discussion in the appendix).

3. BRIEF DESCRIPTION OF MINERAL OILS AND SYNTHETIC OILS*

Mineral oils (the reference) and synthetic oils are normally composed of a base oil and additives (antioxidants, dispersing agents, etc.).

Oils with a synthetic base are made by combining hydrocarbons of low molecular weight by means of chemical reaction to produce compounds of higher molecular weight. Thus, each molecular structure of the fluid is designed and controlled and has predictable properties.

Oils with a mineral base are normally obtained by physical separation or refining. With the exception of hydrogen processing, the original molecules of the crude oil remain unchanged during this process. These oils also contain trace amounts of impurities (e.g., nitrogen, sulphur and metals).

Oils having a synthetic base are obtained from two sources: non-renewable (fossils) and renewable (animal fats and plants). This second option is attractive for the future in that it is not dependent upon the availability of crude oil.

SAE standard J357a classifies synthetic oils as follows:

- synthesized hydrocarbons
- organic esters
- other (e.g., silicons, polyphenolic esters and phosphated esters).

The synthetic oil used for this study has a polyalphaolephin base.

Polyalphaolephins have several advantages and disadvantages compared to mineral oils. We will confine ourselves here to the difference in fuel consumption between the reference oils and synthetic oils, but this does not mean that the durability and interaction between the oil and the drive train do not merit a separate study.

---

* Refer to bibliographical references at the end of this report.

4. THEORETICAL CONSIDERATIONS ON LUBRICATION AND HEAT EXCHANGES IN MOTOR VEHICLE DRIVETRAINS

4.1 Introduction

The appendix contains an analysis of the efficiency η_{SP} of the power train of a road truck. This efficiency is comprised of several elements:

$$\eta_{SP} = \eta_F \cdot \eta_B \cdot \eta_{PO} \cdot \eta_{ROU} \cdot \eta_{JE} \quad (1)$$

where:

η_{SP} - the overall power train efficiency

$$(\eta_{SP} = 1 - \frac{N_R}{N_{SM}})$$

where:

N_R - the power at drive wheels, kW

N_{SM} - the engine output power (engine mounted in truck), kW

η_F - the coefficient for internal friction between gears

η_B - the coefficient for oil churning in various components

η_{PO} - the coefficient for oil pump efficiency (if applicable)

η_{ROU} - the coefficient for friction in bearings

η_{JE} - the coefficient for friction in sealing joints

The losses discussed here are broken down into two main classes:

- losses independent of transmitted torque but dependent solely on road speed (rpm),
- losses dependent on transmitted torque and road (rotating) speed.

The first class includes oil churning, the oil pump and friction in the sealing joints given that these elements depend solely on road (rotating) speed. In other words:

$$\eta_{BH} = \eta_B \cdot \eta_{PO} \cdot \eta_{JE} \quad (2)$$

where:

$\dot{\eta}_{BH}$ = the efficiency with no torque applied

The determination of $\dot{\eta}_{BH}$ is explained in the appendix ($\dot{\eta}_{BH} = 1 - \dot{F}_{BH}/F_{SM}$ and will be discussed further on).

The second class of losses includes friction between the gears and in the bearings, given that these elements are dependent on both road (rotating) speed and transmitted torque. In other words:

$$\eta_{FC} = \eta_F \cdot \eta_{ROU} \qquad (3)$$

where:

η_{FC} = the coefficient for friction as a function of road (rotating) speed and transmitted torque

The determination of this coefficient is explained in the appendix ($\eta_{FC} = 1 - F_{FC}/F_{SM}$) and will be discussed further on.

4.2 General Discussion on Lubrication

Based on the large body of gearworks lubrication data published by researchers (Klamann, 1981), we can draw a number of conclusions concerning the factors affecting the friction coefficients in an environment where oil is in contact with the gears.

- The surface tension between the gear teeth has little effect on the friction coefficient.
- The friction coefficient increases with an increase in oil viscosity.
- The friction coefficient drops with an increase in the rate of slippage between the teeth.
- The friction coefficient is influenced by the temperature of the surfaces in friction, not the oil temperature.
- The friction coefficient also depends on oil composition and additives. Naphta oils, for instance, generate more friction than paraffin oils.

Losses owing to oil churning are basically dependent on oil viscosity. One aim of this study is to explore the effect of viscosity on the power consumption of a road vehicle under actual operating conditions.

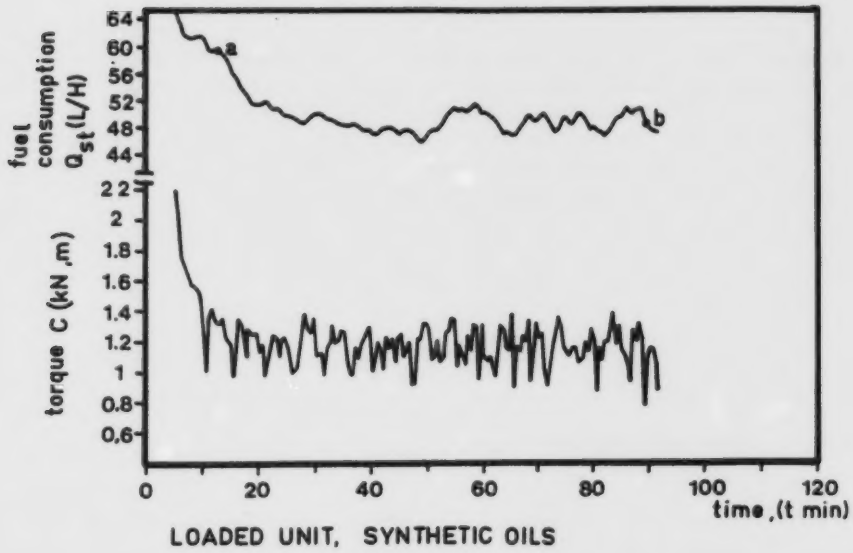

Figure 2 Fuel consumption and torque behind transmission measured during stabilization testing on the test track

Figure 2 plots the drop in energy consumption with the rise in synthetic oil temperatures (Fig. 5) in the engine, transmission and two rear axles of the loaded test vehicle (total mass 46,820 kg) moving around the Blainville track at an average speed of 23 m/sec (83 km/h). It shows a difference of about 17% in fuel consumption between point "a" (10 min into the test) and point "b" (91 min into the test), at which point the temperatures had all but stabilized.

This points up the major effect of viscosity on the power train losses of a road truck.

4.3 Heat Exchange between Oils and Environment

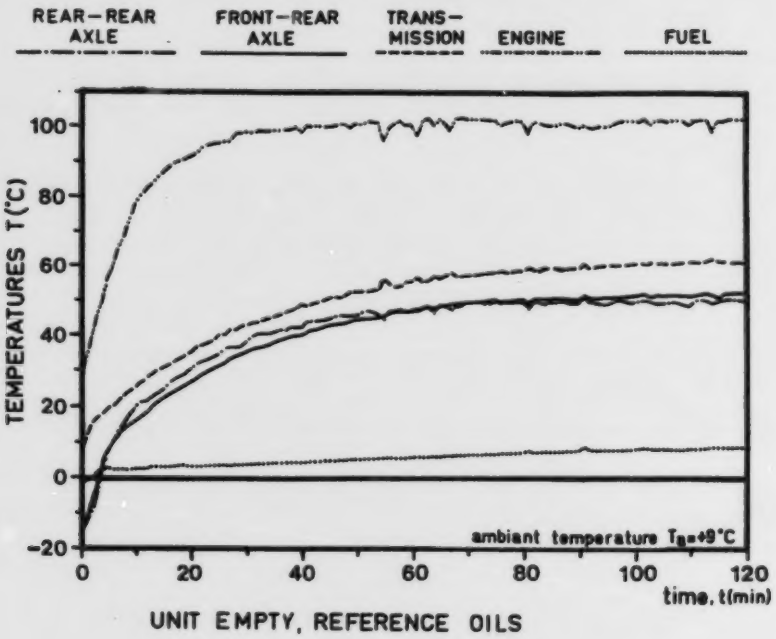

Figure 3 Stabilization test for engine, transmission and rear axle oil temperatures and fuel temperature

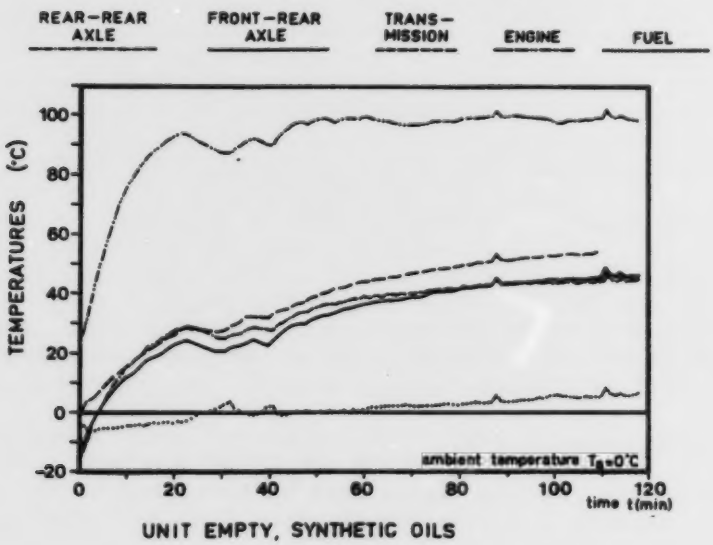

Figure 4 Stabilization test for engine, transmission and rear axle oil temperatures and fuel temperature

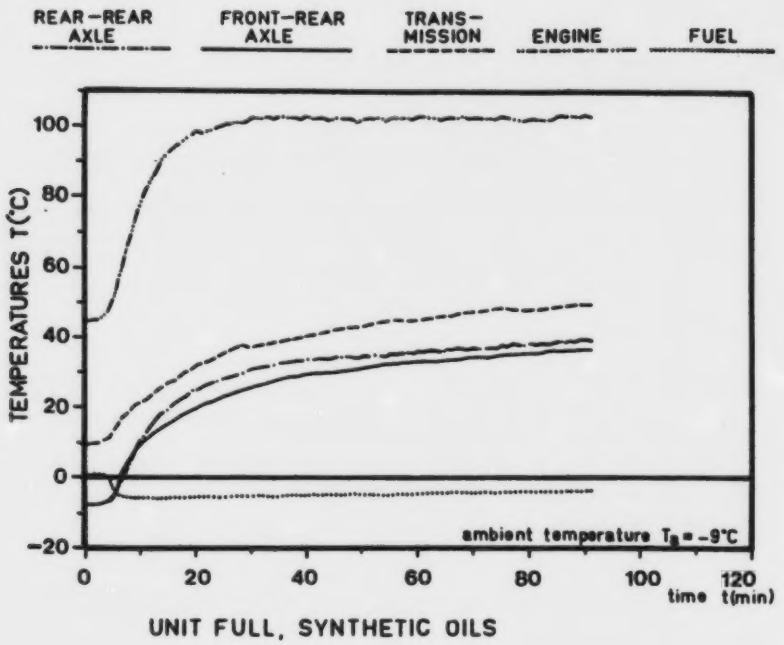

Figure 5 Stabilization test for engine, transmission and rear axle oil temperatures and fuel temperature

Figures 3, 4 and 5 plot temperature movements under the various test conditions.

For a no-load truck-trailer combination, these figures show a gradual rise in temperatures. The temperatures of the oils in the transmission and two rear axles stabilize in about 2 hours. The engine oil and fuel temperatures stabilize in about 30 min.

For a loaded combination, the temperatures of the oils in the transmission and rear axles stabilize in about 80 min and the engine oil and fuel temperatures in about 25 min.

The maximum stabilization temperatures logged for the engine oil range between 100 and 105°C. Those logged for the fuel range between 6 and 20°C whereas maximum stabilization temperatures for the transmission and two rear axles vary from 30 to 60°C, at an ambient temperature of +5°C at no load and -9°C under load.

Referring to formula (91) for a time "t" stretching to infinity (see appendix), we note that the stabilized maximum temperatures of the transmission and two rear axles must be increased by about 15°C in order to make a comparison for the truck at no load and under load.

As a rule, the stabilized maximum temperatures shift in direct relation with the ambient temperatures. Thus, for a given transmission-axle-oil scenario and a given road speed (including the effect of snow, ice and wind) and knowing the stabilized heat balance for a given ambient temperature, we can make a direct determination of the oil stabilization temperatures for any other ambient temperature. In other words, by using formula (91) to determine the overall heat transmission coefficient from direct measurements on the road, we can use this coefficient for any other road scenario.

Figure 4 shows oil temperatures dropping between 20 and 28 minutes after start-up. This is attributable to an unforeseen stop on the test track. The figure shows a substantial drop in temperatures for an 8-minute period, proving that stabilized maximum temperatures are rarely obtained during an irregular duty cycle, which raises fuel consumption even higher with oils of higher viscosity.

Given that the ideal stabilized oil temperatures should lie between 80 and 90°C, stabilized maximum temperatures of about 40°C for the power train are much too low and cause additional fuel consumption.

Thus, the 20% difference between consumption at the start and the end of the run after about 2 hours would be much greater if the temperatures had stabilized at about 80°C. This holds true for both the reference oil and the synthetic oil.

5. TEST RESULTS

5.1 Determination of Oil Churning Losses through the Power Train

In section 4 we showed the distribution of losses through the power train of road trucks. Two classes of losses were identified, the first dependent solely upon road speed (for given oils and a given temperature combination) and the second dependent upon road speed and the torque transmitted by the power train.

The first class, the results for which will be examined here, include losses owing to oil churning, the oil pump in the forward-rear axle and friction in the sealing joints.

The appendix contains a description of the "free-wheeling deceleration" method developed by FERIC. This method calls for testing with the traction wheels of the truck raised off the ground.

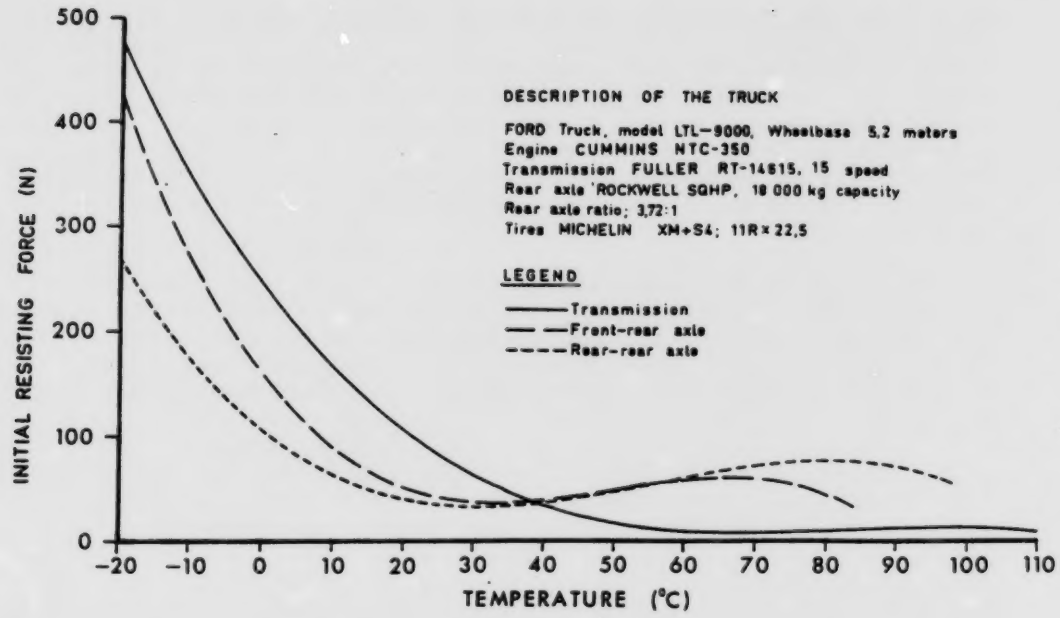

Figure 6. Initial force of resistance owing to oil churning in the transmission and two rear axles as a function of oil temperature--reference oil

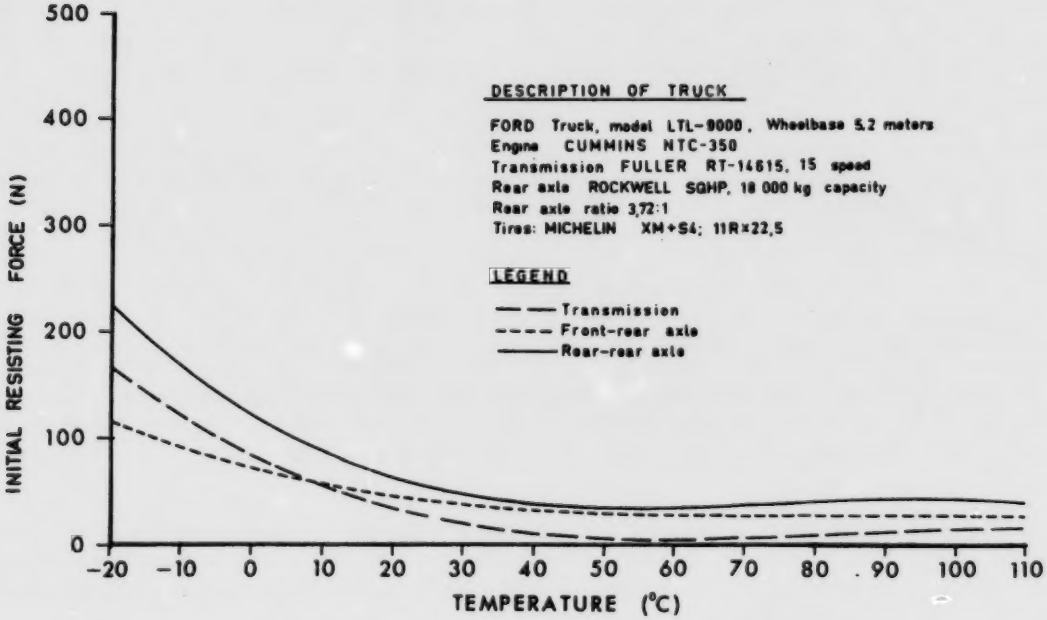

Figure 7 Initial force of resistance owing to oil churning in the transmission and two rear axles as a function of oil temperature--synthetic oil

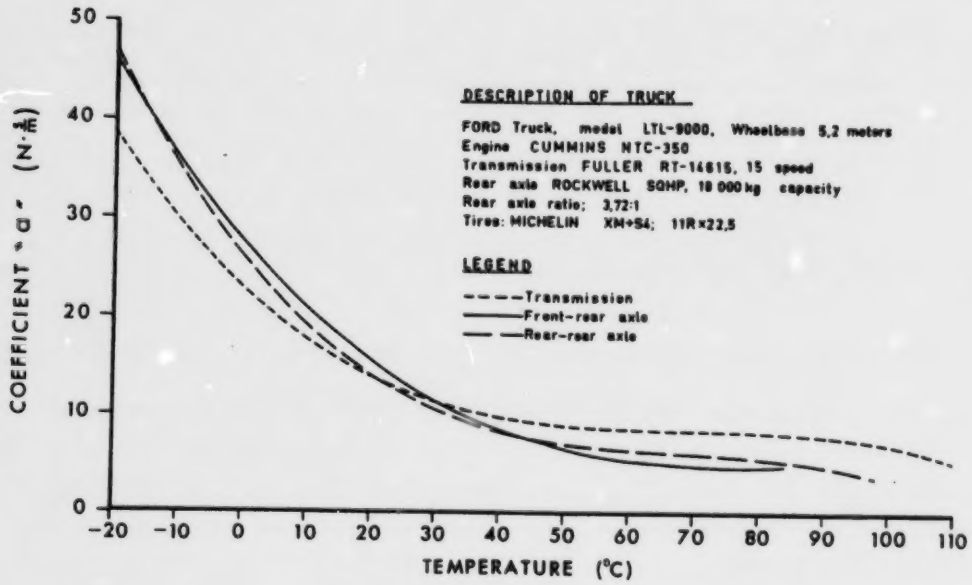

Figure 8 Coefficient "a"* for the reference oil as a function of oil temperature

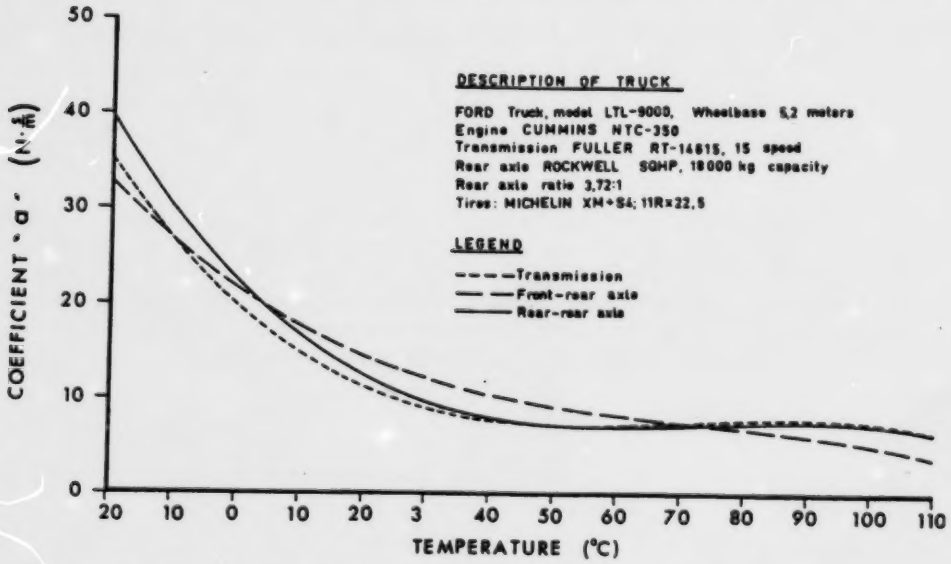

Figure 9 Coefficient "a" for the synthetic oil as a function of oil temperature

---

"a" Coefficient for rate of change of oil churning losses in the transmission and two rear axles.

Using this method and the two test oils, we tested the transmission by itself, then the forward-rear axle and lastly the rear-rear axle. Figures 6 through 9 are graphic representations of the results of those particular tests. Indeed, the study method employed allows us to determine the basic principles necessary for the separate calculation, with any oil temperature in the transmission, forward-rear axle and rear-rear axle, of the coefficient "a" and of the initial force of resistance F_{BH_o}, as they relate to oil churning (including the effect of the oil pump in the forward-rear axle and the oil seals).

The resulting "a" coefficient and the initial force $\dot{F}_{BH_o}$ will be used later during the energy balance analysis and the determination of the resistive forces F_{FC} (F_{FCE}) owing to friction in the power train. To determine the force F_{BHE} and the a_E coefficient, we will use the above figures, adding the values for the two rear axles only (excluding the transmission values).

To calculate the total resistive force $\dot{F}_{BH}$ owing to oil churning in the power train for a given combination of oil temperatures and a given road speed v_r, we will use equation (35) developed in the appendix, i.e.:

$$\dot{F}_{BH} = \dot{F}_{BH_o} + a \cdot v_r \qquad (4)$$

This formula was used to calculate the forces corrected for the traction wheels. Multiplying those values by the speed in m/s, we obtained the power in W or hp (see Fig. 10). Lastly, we read from Figure 11 the corresponding fuel consumptions for the two test oils as a function of oil temperatures for rotating speeds corresponding to road speeds of 80 and 40 km/h. This explains how Figure 12 was established.

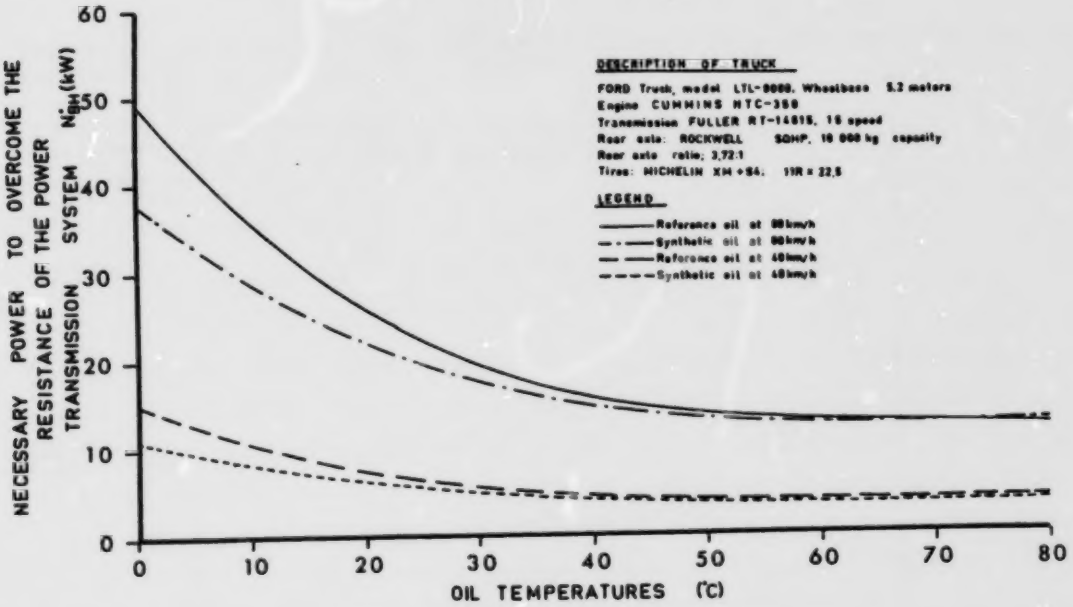

Figure 10 Oil churning resistances in the transmission and two rear axles as a function of oil temperature*

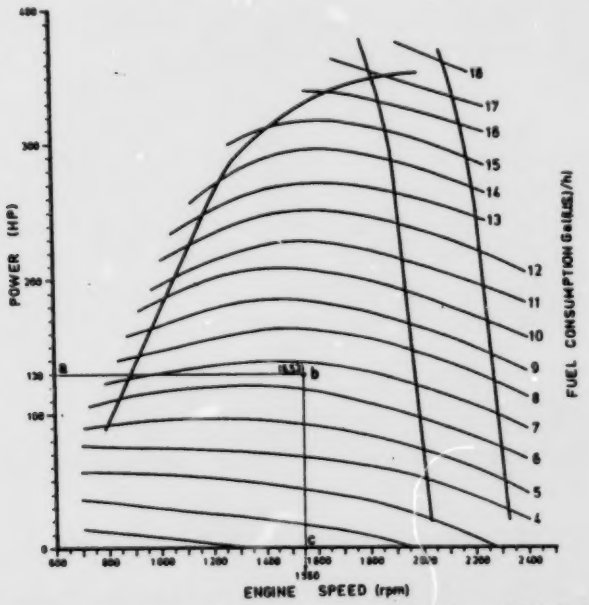

Figure 11 Characteristic curves for Cummins 261 kW (350 hp) engine

* Power calculated on the assumption that the three temperatures were the same.

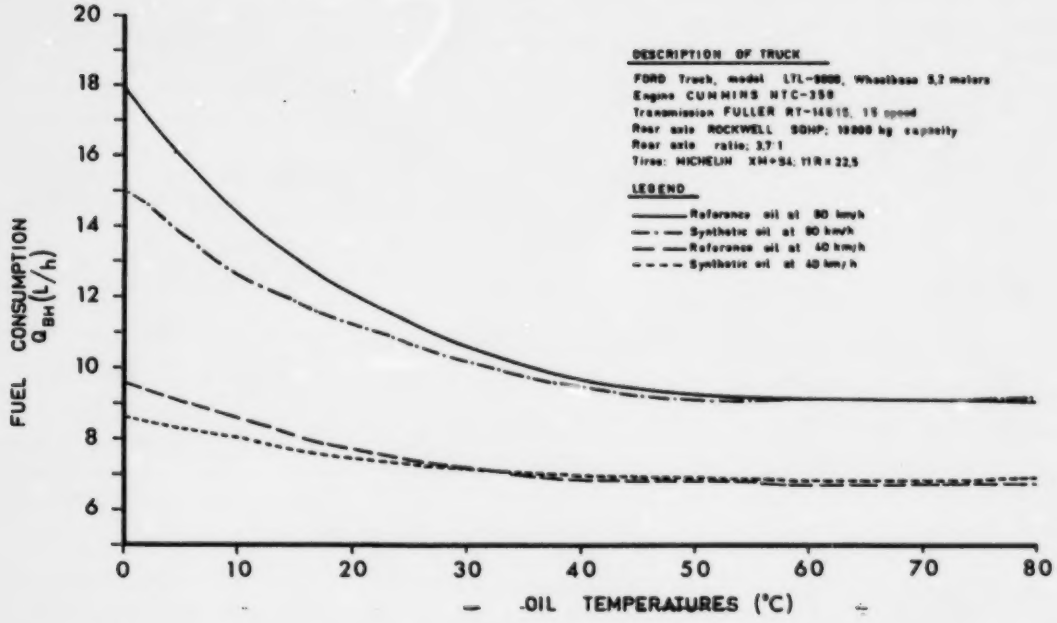

Figure 12 Fuel consumption through oil churning in the transmission and two rear axles as a function of oil temperatures

According to this figure, at 80 km/h and the indicated oils at 45°C, the fuel consumption was about 0.5 L/h lower when the synthetic oil was used. This difference represents about 1.4% of the total on-road truck consumption (at no load and under load) at 80 km/h.

This is attributable to the differences in resistance to churning of the reference oil as compared to the synthetic oil.

The curves presented here show resistances dropping in proportion to the increase in oil temperatures, i.e., with the drop in viscosity. The same can be said for the difference in consumption between the synthetic oils which have lower viscosities than the reference oils at the same temperatures.

5.2 Determination of Losses through Tire Rolling and Air Resistance

The "a" coefficients and the initial resistive force $\dot{F}_{BH_o}$ owing to oil churning in the transmission and two rear axles have just been determined for the two oils.

The force of tire rolling and air resistance F_{A+R} [see equation (54) in section 1.3.3 of the appendix] must now be determined.

The energy balance in this case is expressed by equation (56), given in section 1.3.3 of the appendix and reproduced below:

$$G_T \cdot \delta_A \left(\frac{dv_r}{dt} \pm \frac{g}{\delta_A} \cdot \sin\alpha_p\right) = - F_{TR_o}^{\bullet} - a \cdot v_r - c \cdot v_r^2 \qquad (5)$$

To calculate the energy balance of a vehicle in free-wheeling deceleration, we must first know the δ_A coefficient, which is derived by equation (25) in the appendix. After determining all the components, we obtained coefficient $\delta_A = 1.08$ in the case of the test combination (in free-wheeling deceleration). We were thus able to determine the force F_{TR_o} and the "c" coefficient for each tenth of a second by knowing the δ_A coefficient, the deceleration dv_r/dt (obtained by double derivation of the time-distance relation or simple derivation of the relation $v_r = ds/dt$, both logged on the road, see Fig. 13) and knowing the incline α_p of a portion of the Blainville test track, obtained by profiling the strip every 3 m.

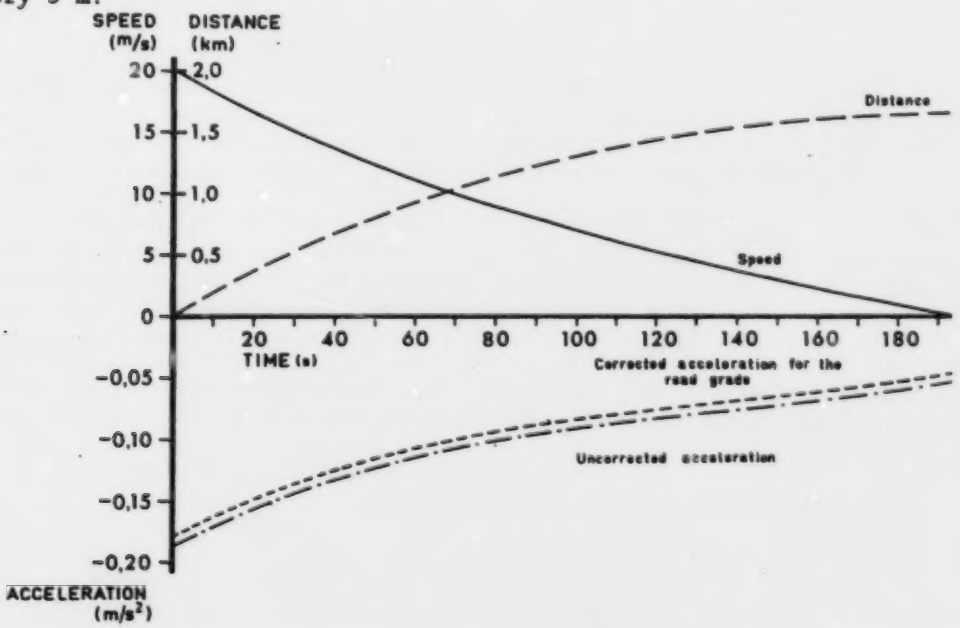

Figure 13 Diagram of distance, speed and acceleration as a function of time (free-wheeling deceleration)

Readers curious to know how these theoretical methods were developed are referred to paragraphs 1.3.3.1 and 1.3.3.2 of the appendix.

The two methods above were used to calculate the initial force $\dot{F}_{TR_o}$ ($\dot{F}_{RR_o} + \dot{F}_{BH_o}$) and the c coefficient. Comparing the total forces in Figure 14, we see that the difference is minimal for the commonly used road speeds, which proves that the two methods are accurate and comparable.

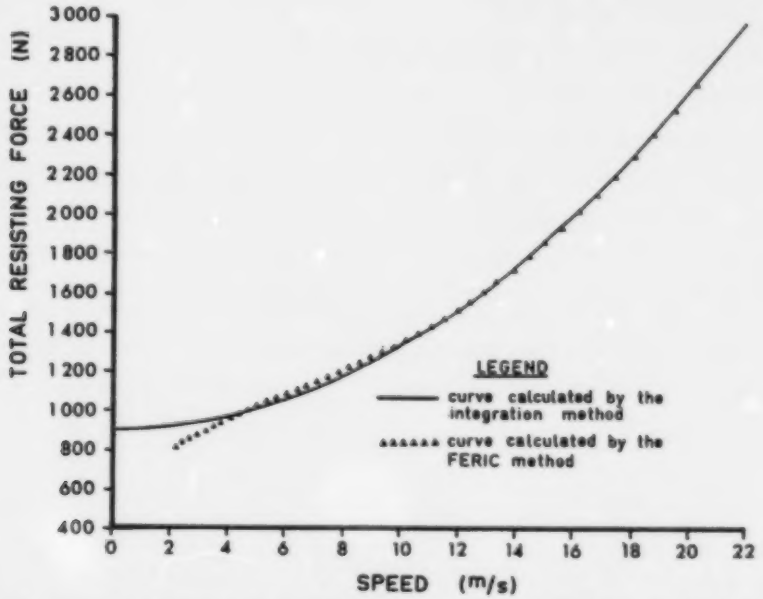

Figure 14 Total forces of resistance for a truck-trailer combination obtained by free-wheeling deceleration as a function of speed

The truck and off-load trailer were tested on the straight portion of the Blainville track, decelerating 13 times in one direction and 13 times in the other. For each test we used the FERIC method to determine the initial resistive force $\dot{F}_{RR_o}$ and the "c" coefficient [see equation (78) in paragraph 1.3.3.2 of the appendix] and then calculated a general average. Those calculations yielded the following results:

c (average) = 5.58 $N \cdot s^2/m^2$; and

$\dot{F}_{RR_o}$ (average) = 867.02 N

Given that the tire rolling resistance is directly proportional to the specific load per tire, the loaded truck with a closed, van-type trailer will have the same air resistance, but the rolling resistance will be directly proportional to the load. In the case at hand, the proportion is 2.93 for the truck weighing 16,000 kg at no load and 46,820 kg under load. The situation for the loaded truck will therefore be

$$c = k + KF = 0.4 \times 2.93 + 5.18 = 6.38 \text{ N}\cdot\text{s}^2/\text{m}^2$$

$$\dot{F}_{RR_o} = 867.02 \times 2.93 = 2540.4 \text{ N}$$

Using this method, we corrected the above values during deceleration for the oil temperatures in the power train.

Having determined the "a" (a_E) and "c" coefficients and the forces $\dot{F}_{BH_o}$ ($\dot{F}_{BHE_o}$) and $\dot{F}_{RR_o}$ ($\dot{F}_{BH_o} + \dot{F}_{RR_o} - \dot{F}_{TR_o}$), we can return to equation (49) in the appendix and calculate the force F_{FCE}, i.e., the force of friction in the two rear axles owing to applied torque. This value will be calculated during the analysis of constant road speeds.

5.3 Analysis of Heat Exchange between Oils and Environment during Temperature Stabilization Testing at Average Speed of 83 km/h, with Comparison of Two Test Oils

These tests were conducted on the Blainville track [all ambient temperatures being very low (-15°C)] at an average speed of 83 km/h until stabilization of the temperatures of oils in the engine, transmission, two rear axles, and the fuel.

The results are given in Figures 3 to 5.

Figure 3 gives the off-load temperature curves for the engine oil and fuel, the transmission oil and the oil in the two rear axles, all oils being the reference types (15W40 in the engine and 80W90 in the transmission and two rear axles). This test was conducted at an ambient temperature of 9°C and lasted about 2 hours. The engine oil stabilized in about 30 min and the other oils in about 2 hours of testing.

The oil temperatures stabilized as follows:

- engine oil ≈100°C
- fuel ≈9°C
- transmission ≈60°C
- two rear axles ≈50°C

Figure 4 gives the off-load temperature curves for the synthetic oils (5W30 in the engine and 75W90 in the transmission and two rear axles). The engine oil stabilized in about 30 min and the other oils within 2 hours. The test was conducted at an ambient temperature of 0°C.

The oil temperatures stabilized as follows:

- engine oil ≈98°C
- fuel ≈6°C
- transmission ≈55°C
- two rear axles ≈46°C

Comparing the temperatures of the two oils, we note that the temperatures of the synthetic oils are slightly lower than those of the reference oils. This is owing to the difference in the ambient temperatures during testing. Turning to the appendix [equation (91)], we see that the ambient temperature has a direct effect on stabilized oil temperatures.

The synthetic oil temperature curves show a drop in temperatures between the 20th and 30th minute of testing as a result of a forced stop on the test track. This proves that as soon as the vehicle stops under actual operating conditions, the temperatures drop, thereby reducing the general averages.

As for temperature stabilization, it can be said that the averages are actually always considerably lower because of rises and dips in the road, as well as stops.

The above tests prove that road trucks in Canada operate with oil temperatures substantially lower than those usually quoted.

The continuous logging of fuel consumption during stabilization testing corresponding to Figures 3 and 4, with an off-load truck and the two oils, shows that the difference in fuel consumption between the moment the engine temperatures stabilize and the driveline oil temperature stabilization is about 8.5%, based on total fuel consumption, with the truck rolling at the stabilization speed.

This difference is comprised of an engine component and a power train component, i.e., they are determined not separately but globally. Further on, we will compare the differences expressed in fuel consumption at the engine and torque measurements behind the torquemeter, representing the losses in the two rear axles for the two oils.

Figure 2 gives the continuous measurements of torque behind the transmission and of the fuel consumption corresponding to the temperatures on Figure 5 for the loaded truck. We observe that consumption and torque drop as the oil temperatures rise, i.e., as viscosities decrease, naturally favouring the oils with lower viscosities at operating temperatures on the road.

5.4 Analysis of Energy Balance on Blainville Track at Constant Road Speeds (20, 40, 60, 80 and 90 km/h) for Two Test Oils

Constant-speed road tests (all temperatures stabilized) represent an ideal means for analyzing the energy balance of a transport vehicle.

To ensure accurate measurements, we drove around the track 5 times clockwise and 5 times counterclockwise and derived the average measurements at each test speed. The results were corrected in the cases where oil or ambient temperatures varied during the test.

The energy balance in this case is represented by formula (49) in the appendix, which is reproduced here in a modified form to match the force of traction at the wheels against the forces of resistance on the road:

$$F_{CMR} - \dot{F}_{BHE} - F_{FCE} = \dot{F}_{RR_o} + c \cdot v_r^2 \pm G_T \cdot g \cdot \sin\alpha_p \qquad (6)$$

In this formula the resistance owing to road incline is eliminated given that tests were conducted in both directions around the Blainville track and that the calculation of the force $\dot{F}_{RR_o}$ and the "c" coefficient take account of the gradient.

The resistive force owing to tire rolling and air drag is given by the following equation [see equation (54) in the appendix]:

$$F_{A+R} = \dot{F}_{RR_o} + c \cdot v_r^2 \qquad (7)$$

Section 5.2 gives the initial force of resistance $\dot{F}_{RR_o}$ and the "c" coefficient (under load and at no load) obtained on the right side of the Blainville test track. Thus, force F_{A+R} in equations (6) and (7) is known.

The force $\dot{F}_{BHE}$ is given by the following equation:

$$\dot{F}_{BHE} = \dot{F}_{BHE_o} + a_E \cdot v_r \qquad (8)$$

where:

$F_{BHE}^{\bullet}$ - the force of resistance through oil churning in two rear axles, N

$F_{BHE_{\bullet}}^{\bullet}$ - the force of resistance at near zero speed through oil churning in two rear axles, N

a_E - the coefficient for rate of change of oil churning losses in two rear axles, N·s/m

The initial force $F_{BHE_{\bullet}}^{\bullet}$ and the a_E coefficient can be determined from Figures 6 through 9.

The torque measured by the torquemeter is corrected for the wheels and converted into the tangential force by the following relation [see equation (31) in the appendix]:

$$F_{CMR} = \frac{M_{CM} \cdot i_{EA}}{r_{CD}^{T}} \tag{9}$$

where:

F_{CMR} - the tangential force obtained by torquemeter measurement and corrected for wheels, N

M_{CM} - the torque measured at torquemeter, N·m

i_{EA} - the rear axle ratio

r_{CD}^{T} - the radius of loaded traction tires with torque applied, m

Thus, [see equation (32) in the appendix], the only unknown in the energy balance is the force F_{FCE} owing to friction resistance in the two rear axles stemming from the application of torque. Isolating this unknown in equation (32) gives:

$$F_{FCE} = F_{CMR} - F_{BHE}^{\bullet} - F_{RR_{\bullet}}^{\bullet} - c \cdot v_r^2 \tag{10}$$

These equations are used to plot curve II for a loaded truck (see Fig. 15), tested in both directions on the track, with synthetic oils in the engine, transmission and two rear axles. This figure also gives the power starting at zero, as well as the power N_{BHE} representing the resistance owing to churning (curve I) and the addition of the two forces (Curve III).

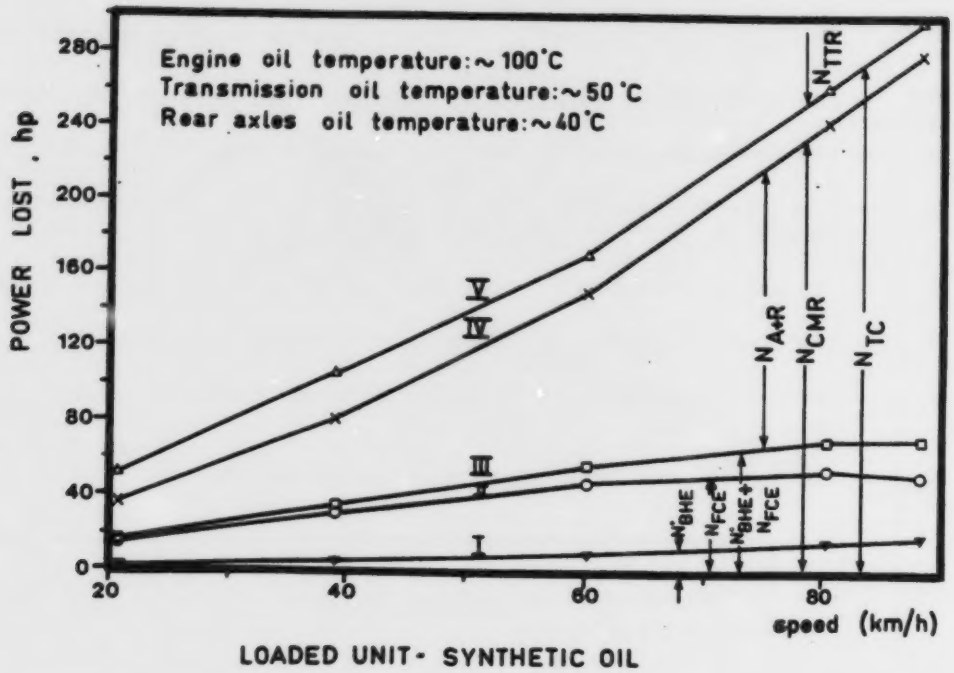

Figure 15 Energy balance on Blainville track obtained by constant speed testing

Interestingly, the resistance owing to applied torque is much greater than the resistance owing to churning at the oil temperatures indicated on the figure.

Curve V represents the total power (hp) necessary to maintain a given speed. It is obtained from the on-road consumption recorded by the FERIC system. The power in hp can be read from Figure 11 for engine rotating speeds (rpm) corresponding to the road speeds. This total power can be expressed by the following relationship:

$$N_{TC} = \dot{N}_{BHE} + N_{FCE} + N_{A+R} + \overbrace{\dot{N}_{BHT} + N_{FCT}}^{N_{TTR}} \qquad (11)$$

where:

N_{TC} - the total power obtained by measured fuel consumption, hp

$N_{BHE}^{\bullet}$ - the power absorbed in two rear axles through oil churning, hp

N_{FCE} - the power absorbed in two rear axles by friction with applied torque, hp

N_{A+R} - the power absorbed by tire rolling and air resistance, hp

$N_{BHT}^{\bullet}$ - the power absorbed by churning of transmission oil, hp

N_{FCT} - the power absorbed by friction in transmission with applied torque, hp

N_{TTR} - the total power absorbed in transmission, hp

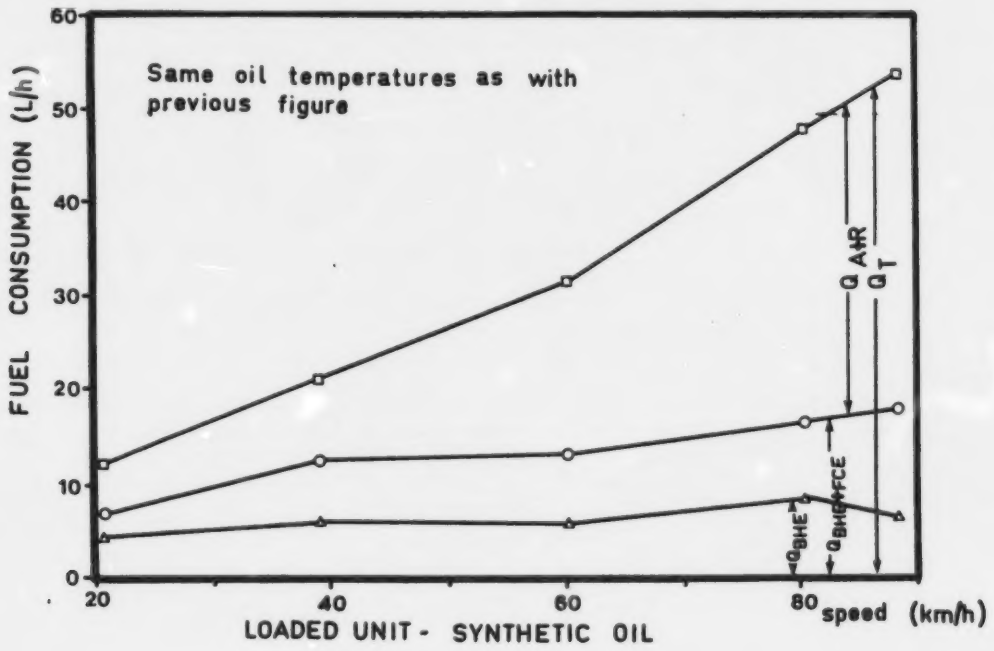

Figure 16 Total energy balance expressed in engine fuel consumption at different speeds

Figure 16 gives the same energy balance but expressed in fuel consumption (L/h) for the various losses.

Figure 17 gives the power train ratings (efficiencies) at average temperatures of 45°C for the synthetic oils in the three components. We note that the rating is 0.70 at 90 km/h and 0.39 at 20 km/h, showing that efficiency drops with a reduction in speed.

The mean efficiency, at 60 km/h for example, is 0.55, considerably lower than the ratings commonly used in the industry for oil temperatures of about 80°C.

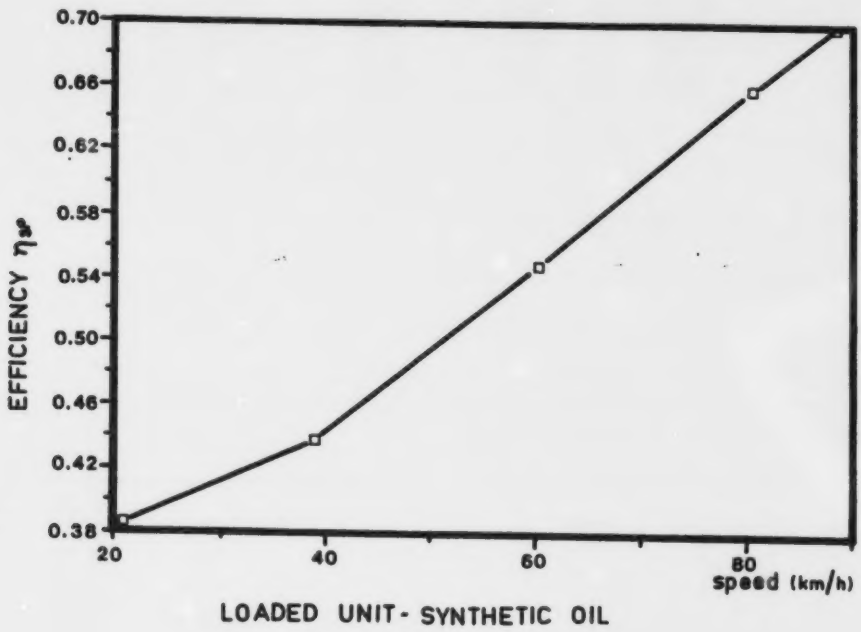

Figure 17 Power train ratings η_{SP} at different speeds

5.5 Comparison of Fuel Consumption with Two Test Oils at Different Constant Speeds

Figure 18 gives total fuel consumptions for the two test oils at no load for speeds of 20 to 90 km/h. Each test entailed driving 5 times around the track in both directions (about 70 km). All fuel consumptions were corrected to the equalized temperatures for respective driveline components.

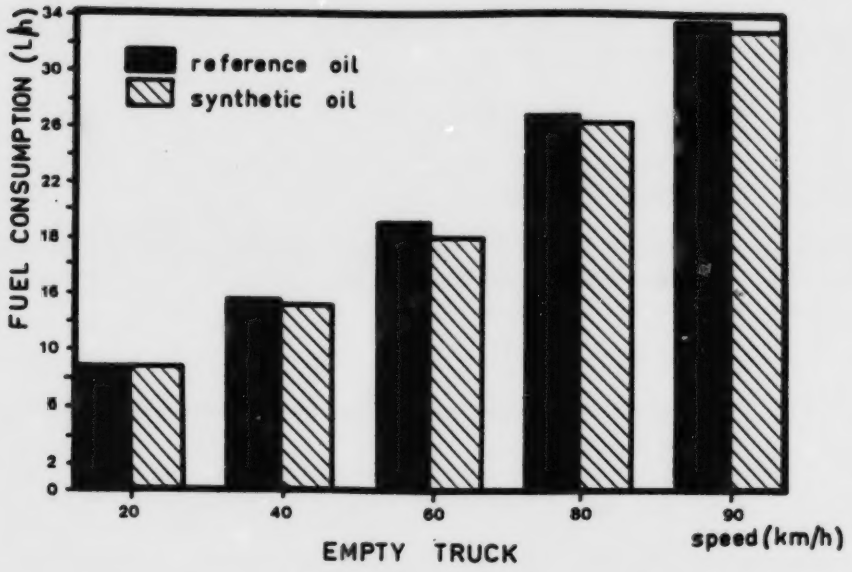

Figure 18 Comparison of total fuel consumption for two test oils as a function of speed

The average difference in consumption at all speeds is 2.74%.

Figure 19 gives total fuel consumptions under load for speeds of 20 to 90 km/h with the synthetic oils and 20, 80 and 90 km/h for the reference oils (same test method).

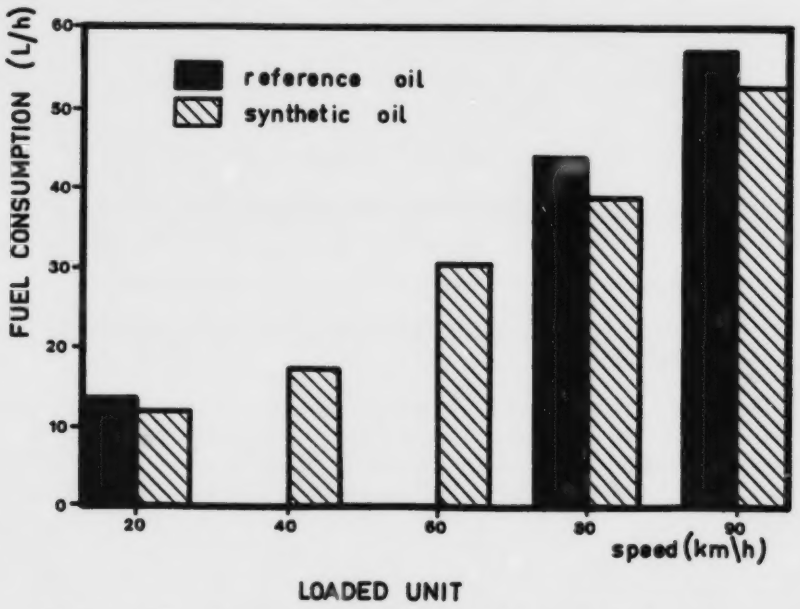

Figure 19 Comparison of fuel consumption for the two test oils as a function of speed

The average difference in consumption at speeds of 20, 80 and 90 km/h is 10.23%.

Thus, the general average under load and at no load is 6.5%.

This difference in consumption includes the engine, transmission and two rear axles. To differentiate between the respective effects of the engine and the power train, we will compare losses in the two axles and the transmission with losses through mechanical friction in the engine.

Mechanical losses with the Cummins NTC-350 engine average 30 hp. Total losses through the transmission and two rear axles average 80 hp (see Fig. 15).

The corresponding fuel consumptions are:
- for 80 hp, 16.28 L/h (obtained on Fig. 11); and
- for 30 hp, 9.27 L/h.

The distribution of consumptions is 62% in the transmission and two rear axles and 38% in the engine. Any difference in consumption between the two oils is therefore to be distributed as above.

5.6 Comparison of Fuel Consumption during Acceleration Testing on Blainville Track

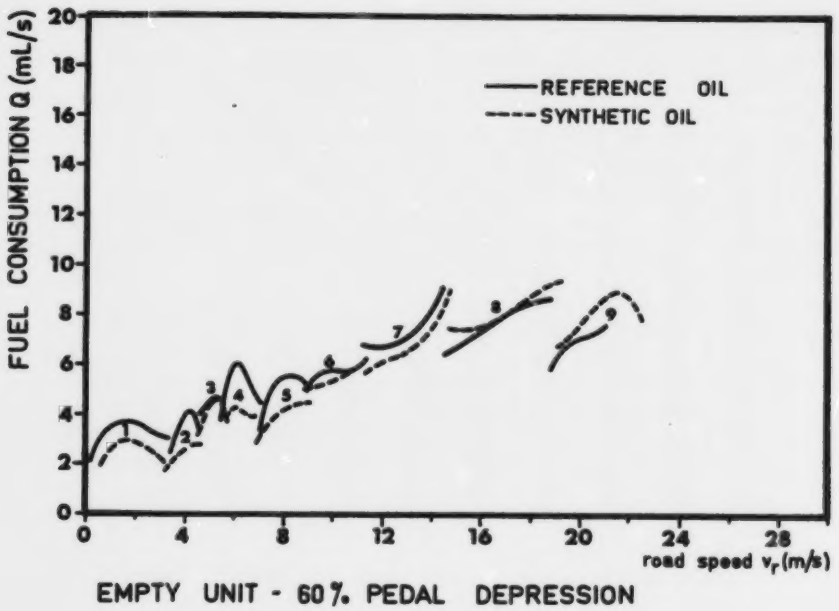

Figure 20 Comparison of fuel consumptions measured in acceleration on the track as a function of road speed (see also Fig. 25)

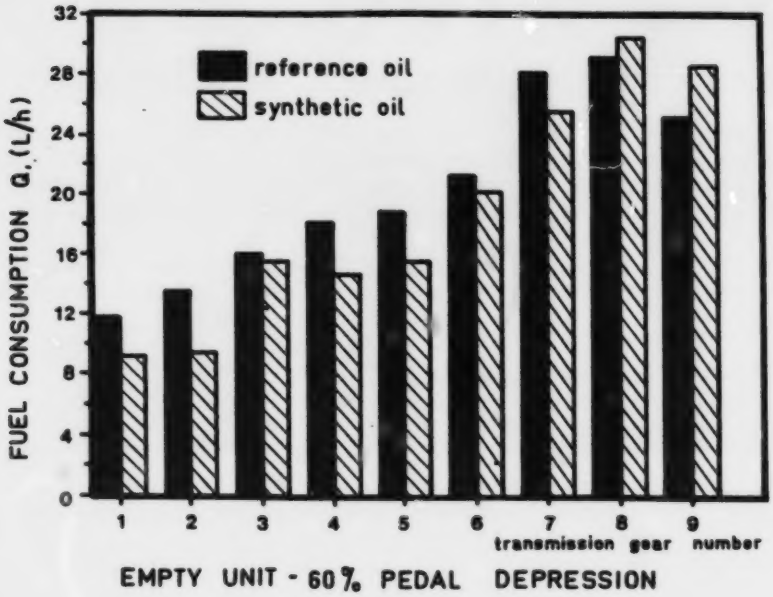

Figure 21 Comparison of fuel consumptions measured in acceleration on the track as a function of transmission ratio

We ran acceleration tests on the right side of the Blainville test track, starting up and shifting through all the gears with the truck off load and the two test oils. These tests were repeated 10 times in both directions for different accelerator positions. Figure 20 shows acceleration with the accelerator at 60% of maximum depression and Figure 21 at 80% of maximum depression. The curves were obtained by polynomial regression from real points. Some distorsion of the curves is evident given that the driver did not use the entire range of engine speeds before shifting to a higher gear. We therefore had to replace this portion by polynomial regression.

The mean difference in fuel consumption (for all ratios) is as follows:

- at 60% accelerator depression, about 7% less fuel was consumed with the synthetic oils than with the reference oils;
- at 80% accelerator depression, about 10% less fuel was consumed with the synthetic oils than with the reference oils.

Figures 22 to 24 are graphic representations of these differences.

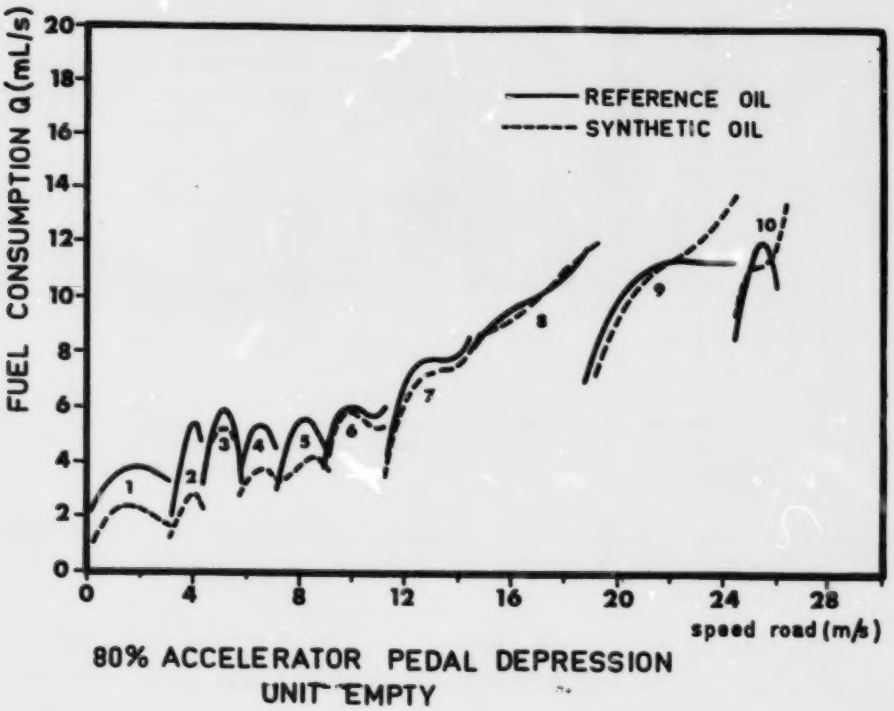

Figure 22 Comparison of fuel consumption for the test oils in acceleration as a function of road speed

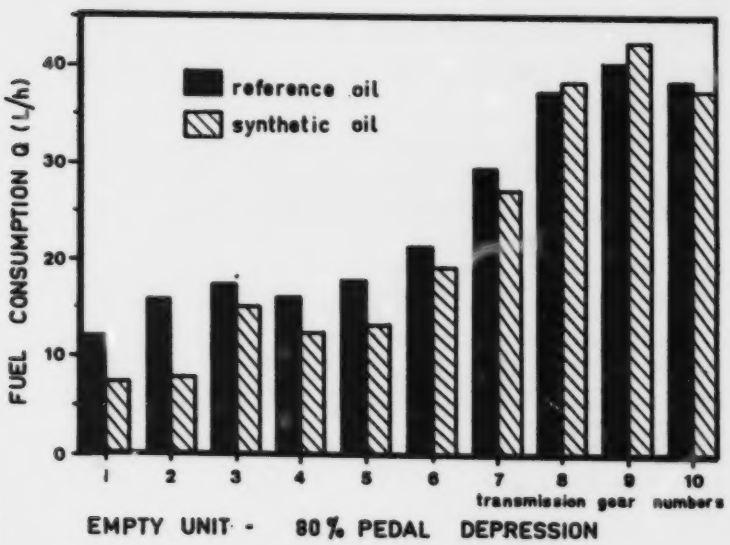

Figure 23 Comparison of fuel consumption for the two test oils in acceleration as a function of transmission ratio

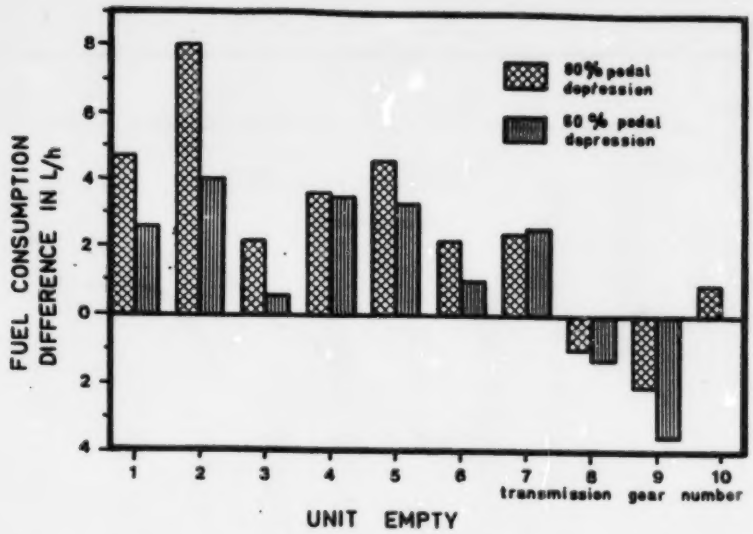

Figure 24 Comparison of differences in fuel consumption for the two test oils in acceleration as a function of transmission ratio

5.7 Comparison of Fuel Consumption for Two Test Oils in Normal Road Duty (Mont-Laurier, Ferme-Neuve, Lac des Écorces, Mont-Laurier)

To compare the results obtained under controlled conditions on the Blainville track, we ran normal-duty road tests in the Mont-Laurier area. Those tests were conducted in both directions over the same distance with the same driver.

As consumption was 56 L/h with the synthetic oils and 59.58 L/h with the reference oils, the difference is 6%.

This corroborates the values obtained under controlled conditions on the Blainville track.

5.8 Analysis of Results

5.8.1 Oil Churning Losses through Power Train

These losses are directly proportional to viscosity. In the case of our two test oils, we had the following viscosities in the power train alone:

reference oil 80W90
at 40°C → 158 cSt
at 100°C → 16.7 cSt
synthetic oil 75W90
at 40°C → 100 cSt
at 100°C → 15.8 cSt

These differences in viscosity caused a difference of about 1.4% in fuel consumption at a road speed of 80 km/h, at oil temperatures of 45°C (loaded and return empty average).

Given oil temperatures of 10°C, for instance, there would be a consumption difference of 4.3% due solely to churning of the oils in the power train (see Fig. 12). These stabilized oil temperatures were obtained with an ambient temperature of about 4.5°C (9°C and 0°C). Referring to equation (91) in the appendix, we note that the stabilized temperatures in the transmission and two rear axles vary in direct relation to the ambient temperature. We realize that the stabilized oil temperatures will be even lower in winter and thus the difference in fuel consumption will be even higher between oils of different viscosities (see Fig. 6 to 9).

Figure 4 shows each stop of the truck reducing the oil temperatures, producing an even greater difference in fuel consumption.

An interesting future study would focus on the development of new lubricants that would produce a more substantial reduction in power losses caused by oil churning in the power train of motor vehicles.

5.8.2 Stabilization Tests

As demonstrated in the appendix, stabilized oil temperatures depend upon the ambient temperature, the square root of the release of heat Q', the square root of the inverse of the total heat transmission coefficient k, and the square root of the inverse of the cooled surface area.

To take an example, the stabilized temperature at a given road speed and with a given power train and oils, will be directly dependent upon the ambient temperature or conditions. In the case at hand, we could use formula (90) to predict the intermediate stabilization temperatures or the stabilized temperatures by having recordings such as those indicated on Figure 3.

Figure 2 shows fuel consumption and torque measured behind the torquemeter dropping during the first 60 minutes of movement, which proves that the oil temperatures have a large impact on the energy consumption and wear of the power train of a vehicle.

Some lubrication experts believe that anti-wear additives with a phosphorus or sulphur base that no longer react with surfaces in friction at temperatures below 60°C cause a substantial increase in transmission wear. If this is true, the results of our study prove that the subject of lubrication merits systematic scientific investigation in future in Canada.

5.8.3 Constant-Speed Road Tests

Observation of Figure 15 prompts the following comments:

- Drive-train resistance owing to oil churning $F_{BH}^{\bullet}$ increases almost linearly with road speeds.

- Drive-train resistance owing to friction F_{FC} with applied torque initially increases linearly (up to 60 km/h) with road speed and then (between 60 and 80 km/h) in a curve to reach a maximum at 80 km/h, after which it drops slightly at 90 km/h. In other words, friction losses are greatest at high speeds (total drive-train resistance for the loaded 46,820 kg truck at 90 km/h amount to about 83 hp).

The power train efficiencies for the loaded truck are given on Figure 17. We note that the efficiency is 0.70 at 90 km/h and 0.39 at 20 km/h for oil temperatures of about 45°C. The figures show that the 0.83 to 0.86 ratings commonly used by assuming the oil temperatures to be 90°C when drafting vehicle specifications are far too high to represent conditions in Canada, particularly in winter.

In a future study, it would be interesting to probe further into the efficiency for various oils, at various temperatures, torques and road speeds for a given vehicle. This would be used to establish better machine specification standards.

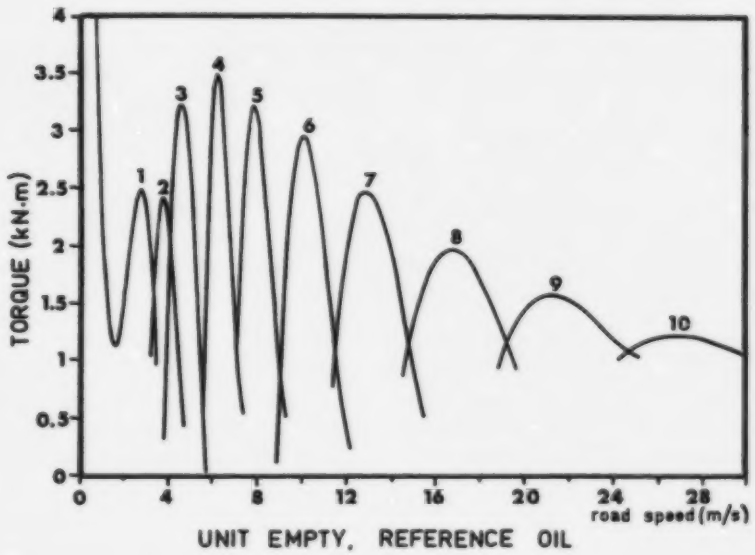

Figure 25 Torque as determined by road speed measured during acceleration testing

Comparison of fuel consumption for the two test oils shows that an oil--either in the engine or the power train--with a lower and flatter viscosity curve through the range of oil temperatures actually experienced would have major advantages in terms of power demand and energy consumption, providing that its anti-wear properties remain the same.

A 6.5% difference in energy consumption between the reference and synthetic oils (under load and at no load) for the range of test speeds proves that it would be very useful for Canada to study this subject in depth, attempting to develop new products even better than 5W30 for the engine and 75W90 for the power train.

The breakdown of the different losses between the engine and the power train being approximately one-third/two-thirds (see p. 27), an in-depth analysis of the engine alone would be desirable in the near future.

5.8.4 Acceleration Testing

We note from Figures 20 and 21 that the differences in consumption increase directly with transmitted torque. For example, the greatest differences (up to 20% between the two oils) occur in fourth gear, which is directly related to transmitted torque (see Fig. 25). With the reduction in torque at the faster ratios, we observe a difference in consumption as well. This proves that the differences in energy consumption depend not only on viscosity but to a greater extent on the lubricating properties of the various oils. In our case, for example, the synthetic oil is superior to the reference oil in terms of lubrication with applied torques. There would be great advantage in exploring the scientific link between torque and losses at constant speeds, for example.

Figure 24 is a graphic representation of the differences in fuel consumption for the two test oils. These differences are 7% at 60% of accelerator depression and 10% at 80% accelerator depression. The fact that these differences are greater than the average difference at constant speeds corroborates the direct relationship between losses and transmitted torque, which is higher in acceleration than at constant speeds (for the same road speed).

5.8.5 Normal-Duty Testing

The difference of about 6% in on-road consumption confirms the accuracy of the measurements made under controlled conditions and thus of FERIC's method of evaluating power losses directly on the road.

6. CONCLUSION

The automatic data logging system which FERIC began developing five years ago was fine tuned and adapted for this study. It provided consistently accurate results as verified through alternative test methods, comparison with theoretical calculations and data from a truck in actual on-road service.

FERIC's theoretical methods of energy evaluation under actual operating conditions have been confirmed by this study, thereby corroborating the results obtained in the past (Fig. 14).

The differences in fuel consumption between the two test oils, obtained under controlled conditions, were confirmed by testing under actual operating conditions. Fuel saving advantages were identified for the synthetic oils both for their lower average viscosities at the temperatures which existed as well as for better lubrication properties which reduced the friction component of the energy transmission losses through the drive train.

The mechanisms governing losses through the power train were broached but would require future analyses.

The oil churning and friction losses were separated, and the proportions were established. Such knowledge will permit the comparative analysis of driveline component designs and materials.

Lastly, the losses due to mechanical friction in the engine were isolated from losses through the power train which will permit future studies to give a better understanding of how an engine performs under actual working conditions and thus identify possible designs or modifications which will improve truck engine performance and efficiency.

APPENDIX

1. DETERMINATION OF POWER LOSSES OF A TRANSPORT VEHICLE ON THE ROAD

1.1 Foreword

FERIC Technical Reports TR-53, TR-55 and TR-61, published in 1982, 1984 and 1985, respectively, investigated the energy balance of a vehicle on the road and explored the means of determining selected factors of this balance. Indeed, it was necessary to quantify the impact of a given factor on the performance and fuel consumption of a transport vehicle (e.g., the impact of different tire inflation pressures on the fuel consumption of a truck-trailer combination, all other conditions being equal). Naturally, those investigations were to be made directly at the transportation sites, without the need to depend on laboratory testing.

With this in mind, we developed methods that, under our particular conditions, should provide for accurate, realistic analysis of one or more components of the energy balance. We have been working for more than four years to fine tune these methods. In this report, while describing the theoretical bases of energy balance, we describe in the following, the latest versions* of the methods of determining the power elements of a road vehicle.

1.2 General Description of Vehicle Energy Balance

The energy balance of a truck-trailer combination is represented by the balance of the external and internal resistive forces acting against the force exercised at the ground by the traction wheels at a given road speed and location. A vehicle combination, considered as a fixed value (at the instant of evaluating the energy balance) undergoes numerous resistances to forward motion, the most important of which are acceleration inertia; tire rolling resistance (including all contributory factors, e.g., tire inflation pressure, configuration and type, road surface and turns, truck and trailer axle spacing, and road gradient), air drag (including wind), and total power train resistance.

---

* These versions are entirely original and currently unique in the world.

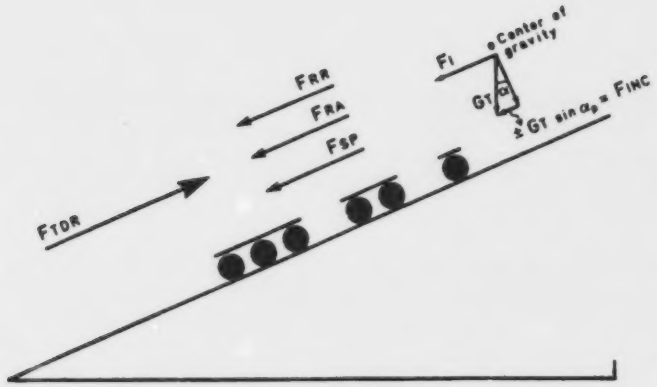

Figure 26 Energy balance of forces acting on a transport vehicle.

Figure 26 diagrams the forces acting on a truck-trailer combination at the given time on the road. The general equation for these forces can be written as

$$F_{TDR} = F_{SMD} - F_{SP} = F_{DRR} \cdot \cos\alpha_p + F_{RA} \pm F_I \pm F_{IR} \pm F_{INC} \qquad (12)$$

where:

F_{SMD} - the dynamic drive force at engine output, N

F_{TDR} - the total dynamic traction at traction wheels (including force of inertia upon acceleration or deceleration), N*

---

* The difference between the force at the ground contact of the drive wheels and the reading from the torquemeter mounted between the transmission and the two rear axles of the test truck will yield the total losses in the two axles, i.e., the corresponding force of resistance F_{SPE}, for the two axles alone (transmission losses are automatically taken into account since the torquemeter is mounted behind the transmission).

F_{DRR} - the dynamic force of tire rolling resistance (including all rolling resistance factors identified in FERIC Technical Report TR-55, D.9.1), N

F_{RA} - the dynamic force of air resistance (including effect of wind), N

F_{SP} - the dynamic force of power train resistance (including oil churning and friction under the effect of transmission torque and speed), N. The study of this force for two different oils is the focus of this project.

F_{I} - the force of vehicle inertia (acceleration or deceleration), N

F_{INC} - the directional force of resistance owing to vertical gradient in the road, N. It equals $g \cdot G_T \cdot \sin\alpha_D$ where G_T is total vehicle mass in kg, α_D is angle of road incline and g is gravitational acceleration.

F_{IR} - the force of wheel and drivetrain inertia, N

For purposes of analysis, this energy balance, presented here in its most general form, must be developed in further detail (based on traditional theories and the experience of researchers around the world). We will attempt to corroborate existing theories through direct measurements.

First of all, we consider the total dynamic force of tire rolling resistance of a truck-trailer combination F_{DRR}, which equals

$$F_{DRR} = \overset{\bullet}{F}_{RR} + F_M + F_\delta + F_C + F_{SD} + F_{SC} + F_{IR} \qquad (13)$$

where:

$\overset{\bullet}{F}_{RR}$ - the force of rolling resistance on ideally flat, straight road without applied torque (traction), N. Superscript "•" designates zero traction torque, N. This force will be analyzed further on in the section on free-wheeling deceleration.

The force $\overset{\bullet}{F}_{RR}$ is given by the following formula:

$$\overset{\bullet}{F}_{RR} = \overset{\bullet}{F}_{RR_o} + k \cdot v_r^2 \qquad (14)$$

where:

$\dot{F}_{RR_0}$ - the force of rolling resistance at near zero speed, N

k - the coefficient for rate of change of rolling resistance losses as a function of squared speed, $N \cdot s^2/m^2$

v_r - the road speed, m/s

Analysis of the initial force $\dot{F}_{RR_0}$ and the "k" coefficient will be explained further on. But first, we will consider that the forces F_δ, F_C, F_{SD}, F_{SC} and F_{IR} will be included in the force $\dot{F}_{RR}$, given that we will make comparative tests (always with the same unit on the same road).

F_M - the additional force owing to application of torque at drive wheels, N. This force is calculated by the following formula:

$$F_M = \frac{F_{TDR} \cdot (\dot{r}_{CD} - r^T_{CD})}{G_T \cdot \dot{r}_{CD}} \qquad (15)$$

where:

G_T - the total vehicle mass, kg

$\dot{r}_{CD}$ - the radius of loaded traction tires without applied torque, m

Radii $\dot{r}_{CD}$ and r^T_{CD} can be calculated by approximate empirical formulae or by direct summation of the revolutions of the traction wheels for a strip of road of predetermined length. From this we extract the radius.

Through free-wheeling tests, we determine the kinematic radius (without applied torque). Testing with applied torque, we will obtain the dynamic radius.

F_δ - the force of rolling resistance owing to angle of side slip of front (drive) wheels, N and appears at the moment the truck negotiates a curve. The determination of this force as a function of road curvature is the subject of another project which FERIC has undertaken with Transport Canada.

F_{SD} - the force of rolling resistance owing to ground deformation, N. This resistance as a function of permanent road deformation is analyzed in a special project currently under way at FERIC.

F_C - the force of rolling resistance owing to camber of forward (drive) wheels, N

F_{SC} - the force of rolling resistance owing to suspension type and vibration, N. This resistance will be analyzed in forthcoming FERIC studies.

We will next consider the total dynamic force of air resistance F_{RA} (including wind direction and velocity).

This force is given by the following equation:

$$F_{RA} = K \cdot S_C \cdot (v_r^v)^2 \cdot \cos\theta \qquad (16)$$

where:

K - the coefficient for rate of change of air drag losses as a function of squared speed, $N \cdot s^2/m^4$

S_C - the corrected vehicle frontal area, m^2

v_r^v - the road speed corrected for wind velocity, m/s

θ - the angle of wind direction relative to vehicle longitudinal axis, degree

This force will be examined later on in this report.

Indeed, as the main purpose of this study is to compare the dynamic resistance losses of the power train (drivetrain) represented by the force F_{SP}, this is the value which must be isolated in each case.

It is comprised of the force of resistance owing to oil churning in the transmission and two axles (including friction inherent in the sealing joints and bearings without applied rotating torque) and the force owing to friction generated by applied rotating torque. It can therefore be written as follows:

$$F_{SP} = \dot{F}_{BH} + F_{FC} \qquad (17)$$

where:

$\dot{F}_{BH}$ - the total force of resistance to churning without applied torque, N. Comprised of initial force of churning resistance (upon starting) and an effort varying linearly with vehicle road speed; its equation is as follows:

$$\dot{F}_{BH} = \dot{F}_{BH_\bullet} + a \cdot v_r \tag{18}$$

where:

$\dot{F}_{BH^\bullet}$ - the initial force of resistance to churning where superscript "°" designates zero torque and subscript "•" designates near zero speed, N

a - the coefficient for rate of change of oil churning losses in transmission and two rear axles, N•s/m

F_{FC} - the force of resistance owing to power train friction with applied drive torque, N

Further on, we will deal with the method established to determine the forces represented by equations (17) and (18).

The force of wheel and power train inertia F_{IR} corrected for the wheels equals

$$F_{IR} = \frac{\left(\Sigma^{n} J_R + J_{SP}\right)}{\left(r_{CD}^{T}\right)^2} \cdot \frac{dv_r}{dt} \tag{19}$$

where:

J_R - the moment of inertia of a tire with its rim, kg•m². (The method of determining this moment of inertia is explained on page 48.)

J_{SP} - the power train moment of inertia, kg•m²

j_{as} - dv_r/dt - vehicle translational acceleration, m/s²

The force of vehicle inertia F_I [excluding the force (F_{IR})] is equal to:

$$F_I = G_T \cdot j_{as} = G_T \cdot \frac{dv_r}{dt} \tag{20}$$

The force of engine rotating inertia corrected for the wheels is equal to

$$F_{IRM} = J_M\left(\frac{i_{TR} \cdot i_{EA}}{r^T_{CD}}\right) \cdot \eta_{SP} \cdot \frac{dv_r}{dt} \tag{21}$$

where:

F_{IRM} - the force of resistance through engine inertia, N

i_{TR} - the transmission ratio

J_M - the engine moment of inertia, kg·m²

η_{SP} - the total power train efficiency, equal to

$$\eta_{SP} = 1 - \frac{N_R}{N_{SM}} \tag{22}$$

where:

N_{SM} - is the engine output power (engine mounted in truck), kW

Combining the two forces of inertia yields:

$$F_I + F_{IR} = G_T \frac{dv_r}{dt} + \frac{(\Sigma J_R + J_{SP})}{(r^T_{CD})^2} \cdot \frac{dv_r}{dt} \tag{23}$$

from which:

$$F_I + F_{IR} = G_T \frac{dv_r}{dt} \left[1 + \frac{(\Sigma J_R + J_{SP})}{G_T (r^T_{CD})^2}\right] \tag{24}$$

Designating

$$1 + \frac{\Sigma J_R + J_{SP}}{G_T (r^T_{CD})^2} \quad \text{by } \delta_A \tag{25}$$

gives:

$$F_I + F_{IR} = \delta_A \cdot G_T \cdot \frac{dv_r}{dt} \tag{26}$$

where:

δ_A = the coefficient for vehicle rotating masses

To obtain the total force of inertia with the engine as part of the power train, we add the three forces of inertia and obtain

$$F_{IRM} + F_I + F_{JR} = G_T \cdot \frac{dv_r}{dt} \left\{ 1 + \frac{J_M}{G_T} \left[\frac{i_{TR} \cdot i_{EA}}{r^T_{CD}} \right]^2 \cdot \eta_{SP} + \frac{\sum^n J_R + J_{SP}}{G_T (r^T_{CD})^2} \right\}$$

where the expression in brackets is designated by δ_{AD}, i.e.:

$$\delta_{AD} = 1 + \frac{J_M}{G_T} \left[\frac{i_{TR} \cdot i_{EA}}{r^T_{CD}} \right]^2 \cdot \eta_{SP} + \frac{\sum^n J_R + J_{SP}}{G_T (r^T_{CD})^2} \tag{27}$$

where:

δ_{AD} = the dynamic coefficient for calculating all rotating and translational masses, including engine

Lastly, we must take account of the force caused by negotiating an incline or decline in the road. This force is given by the following equation:

$F_{INC} = \pm G_T \cdot g \cdot \sin\alpha_p$ (see energy balance figure)

where:

α_p = the angle of road incline, degrees

g = the gravitational acceleration, m/s^2

The plus sign (+) designates an incline and the minus (-) sign a decline.

Returning to equation (12) of the energy balance given previously and introducing the developments discussed here, we will have:

$$F_{MD} - F_{SP} = F_{TDR} = [F_{RR_o} + k \cdot v_r^2 + \frac{F_{TDR}\,(r_{CD}^{\cdot} - r_{CD}^{T})}{r_{CD}^{\cdot}}] \cos\alpha_p +$$

$$+ K \cdot S_C \cdot (v_r' \cos\alpha)^2 \pm G_T \cdot \delta_{AD} \cdot \frac{dv_r}{dt} \pm g \cdot G_T \cdot \sin\alpha_p \qquad (28)$$

To analyze the energy balance of a combination on the road, we must determine each of its elements at any given moment. In other words, by fixing all the elements except one, we can not only study it in its natural environment, but also explore how the other elements affect its performance.

We will describe here the methods of determination which FERIC has developed in the past five years. Note that this procedures requires no laboratory.

1.3 Methods of Determining Energy Balance Components for Truck-Trailer Combination

1.3.1 Determination of Force F_{TDR} between Traction Wheels and Ground

Instant determination of the force F_{TDR} acting between the traction wheels and the ground is by no means a simple process. If we measure the fuel consumption, we determine the total loss, including the thermodynamic, thermal and mechanical engine losses, as well as the power train losses. If, on the other hand, we attempt to find the traction force by determining and totaling all energy balance components on the road, the task becomes almost insurmountable without recourse to the laboratory.

FERIC therefore decided to mount a torquemeter between the transmission and the forward-rear axle. Basically, this is an instrument which, featuring greater accuracy (±0.2% of possible error), records as rapidly as required the positive or negative moment transmitted between the transmission and the rear train.

It was FERIC's intention to determine simultaneously the moment from the engine through the transmission and the moment required to maintain a certain speed with a given combination on any given strip of road.

For example, the dynamic moment at the engine output will equal

$$M_M = M_{CM} + M_{PT} \qquad (29)$$

where:

M_M - the dynamic engine rotating moment under variable operating conditions, N·m

M_{PT} - the moment corresponding to total transmission losses (through oil churning and friction), N·m

Formula (29) can be expressed as follow:

$$M_{CM} = M_M - M_{PT} \tag{30}$$

If having measured this torque, we return to the engine fitted with its accessories, we can read the consumption as a function of torque and engine speed (knowing the transmission ratio). On Figure 11 for example, power* of 130 hp at an engine speed of 1550 rpm gives a fuel consumption of 29.65 L/h.

Given that FERIC makes continuous measurements of the total engine consumption of a truck-trailer combination, we can at any given moment determine the consumption corresponding to all the dynamic losses on the road behind the torquemeter, and thus control the addition of all the loss factors determined by mechanical methods (to be described later).

Thus, to avoid having to determine the dynamic force on the road at each instant, we will replace that force by the measurement obtained at the torquemeter corrected for the traction wheels and the losses in the two axles. This gives

$$\underbrace{\frac{M_{CM} \cdot i_{EA}}{r_{CD}^{T}}}_{F_{CMR}} - \dot{F}_{BHE} - F_{FCE} = F_{TDR} \tag{31}$$

---

* This power is obtained from engine moment and speed by formula $M = N/\omega$ or $N = M \cdot \omega \left(\frac{n \cdot \pi}{30}\right)$, n being engine rpm.

or:

$$F_{CMR} - \dot{F}_{BHE} - F_{FCE} = F_{TDR} \tag{32}$$

where:

F_{FCE} - the total force of rotating resistance in two rear axles owing to applied torque (friction), N

Substituting equation (32) in the general energy balance equation (28) will give

$$F_{MD} - F_{SP} = F_{CMR} - \dot{F}_{BHE} - F_{FCE} = [\dot{F}_{RR_o} + k \cdot v_r^2 +$$

$$+ \frac{F_{CMR} - \dot{F}_{BHE} - F_{FCE}\,(\dot{r}_{CD} - r_{CD}^T)}{\dot{r}_{CD}}] \cdot \cos\alpha_p +$$

$$+ K \cdot S_C \cdot (v_r^v \cos\theta)^2 \pm G_T \cdot \delta_{AD} \cdot \frac{dv_r}{dt} \pm g \sin\alpha_p \tag{33}$$

We thus eliminate the need to know the dynamic force of traction at the traction wheels.

The balance given by the above equation can now be examined in detail.

1.3.2 Determination of Force F_{SP} of Power Train Rotating Resistance owing to Oil Churning and Friction, N

This force is comprised of the following components [see equation (17)]:

$$F_{SP} = \dot{F}_{BH} + F_{FC} \tag{34}$$

Since

$$\dot{F}_{BH} = \dot{F}_{BH_o} + a \cdot v_r \tag{35}$$

we have:

$$F_{SP} = \dot{F}_{BH_o} + a \cdot v_r + F_{FC} \tag{36}$$

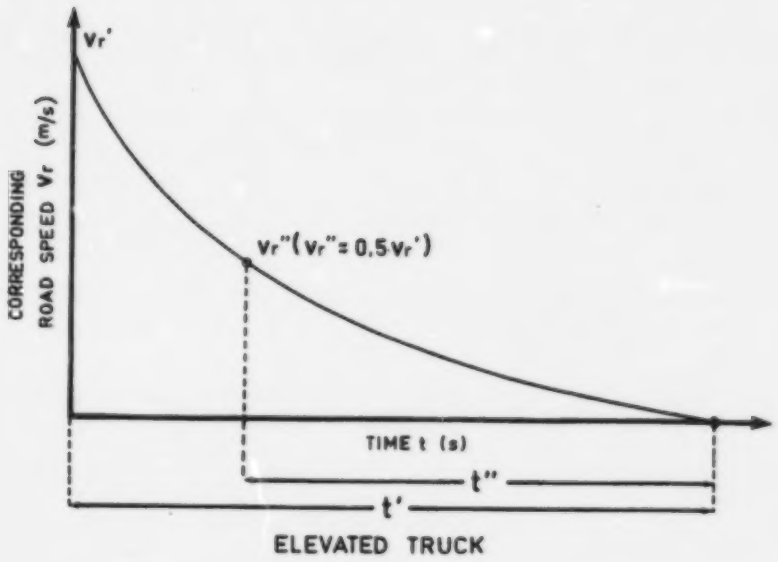

Figure 27 Speed-time diagram obtained by power train deceleration from speed v_r' to zero

1.3.2.1 Analysis of Force $\overset{\circ}{F}_{BH}$

We will start by considering the force $\overset{\circ}{F}_{BH}$. This can be done with the truck raised (wheels off the ground), using the "coast down" or "free-wheeling" method. If we start with the engine connected to a power train, raise the speed to about 70 km/h, and disconnect the engine from the power train, we will obtain deceleration to zero speed. Logging the speed-time relationship will give a curve of the form shown in Figure 27.

Taking the energy balance equation:

$$J \cdot \frac{1}{(\overset{\circ}{r}_{CD})^2} \cdot \frac{dv_r}{dt} = - \overset{\circ}{F}_{BH_o} - a \cdot v_r = - \overset{\circ}{F}_{BH} \qquad (37)$$

where:

J - the combined moments of inertia of traction wheels and power train, $kg \cdot m^2$

and integrating, we obtain

$$t = \frac{J}{a \cdot (\dot{r}_{CD})^2} \cdot \ln \left[\frac{a v'_r + \dot{F}_{BH_o}}{a v''_r + \dot{F}_{BH_o}} \right] \tag{38}$$

where:

v'_r - the initial road speed, m/s

v''_r - the intermediate deceleration speed, m/s

t - the deceleration time from speed v'_r to speed v''_r, s

If we introduce speed $v''_r = 0$ in formula (38) and then simplify, we obtain the equation for the initial force $\dot{F}_{BH_o}$:

$$\dot{F}_{BH_o} = \frac{a \cdot v'_r}{e^{\left(\frac{t \cdot (\dot{r}_{CD})^2}{J} \cdot a\right)} - 1} \tag{39}$$

If based on two speeds v'_r et v''_r we measure deceleration times t' and t" to zero, we obtain the following equation:

$$e^{\left[\frac{t' \cdot (\dot{r}_{CD})^2}{J} \cdot a\right]} = \frac{v'_r}{v''_r} \left[e^{\left[\frac{t'' \cdot (\dot{r}_{CD})^2}{J} \cdot a\right]} - 1 \right] + 1 \tag{40}$$

Equation (40) cannot be solved algebraically. Thus, knowing speeds v'_r and v''_r and the times required to decelerate from v'_r (v''_r) to zero, the "a" coefficient can be found by iteration. Once the "a" coefficient has been found, formula (39) can be used to determine the initial force $\dot{F}_{BH_o}$ starting from a speed of, say, 5 m/s and using the time between 5 m/s and zero.

To calculate the "a" coefficient and the initial force $\dot{F}_{BH_\bullet}$ we must know the radius $\dot{r}_{CD}$ and the power train moment of inertia $J = \sum^{n} J_R + J_{SP}$. At this point, the method for determining this moment of inertia can be developed.

1.3.2.2 Analysis of Moment of Inertia J

As has just been indicated, the moment J is comprised of two elements:

$$J = \sum^{n} J_R + J_{SP} \tag{41}$$

where:

$\sum^{n} J_R$ - total moment of traction wheels, $kg \cdot m^2$

We will first develop a method for determining the moment J_R.

1.3.2.3 Determination of Moment J_R

The diagram below is used to determine the moment of inertia of a wheel moving around its rotating axis on a decline.

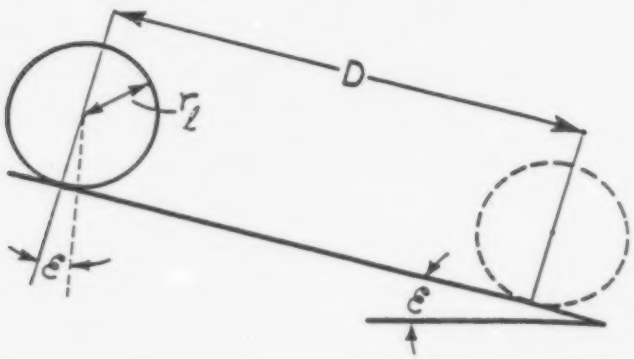

Figure 28 Diagram of wheel rotation on a decline

where:

a_m - wheel acceleration, m/s^2

G_R - mass of wheel with tire, kg

D - distance, m

t_s - time to travel distance D, s

r_1 - free tire radius, m

Force of acceleration $F_a = G \cdot \sin\varepsilon$

The force of inertia equals:

$$F_a = G_R \cdot a_m \tag{42}$$

The force of acceleration is equal to

$$F_a = \frac{2 \cdot G_R \cdot D}{t_s^2}, \text{ since } D = \frac{1}{2} a_m \cdot t_s^2$$

The relative inertia to overcome equals

$$F = J_R \cdot \frac{a_m}{r_1^2} \tag{43}$$

Thus,

$$F = G_R \cdot \sin\varepsilon = \frac{2 \cdot G_R \cdot D}{t_s^2} + \frac{2 \cdot J_R \cdot D}{r_1^2 \cdot t_s^2} \tag{44}$$

from which

$$G_R \cdot \sin\varepsilon = \frac{2 \cdot G_R \cdot D}{t_s^2} \left[1 + \frac{J_R \cdot g}{r_1^2 \cdot G_R}\right] \tag{45}$$

and

$$J_R = r_1^2 \cdot G_R \cdot \left[\frac{g \cdot t_s^2 \cdot \sin\varepsilon}{2 \cdot D} - 1\right] \qquad (46)$$

This formula was used to determine the moment of inertia of one wheel. Multiplying that result by the number of traction wheels gives ΣJ_R.

We then used the method described below to determine the power train moment of inertia.

1.3.2.4 Determination of Moment J_{SP}

This moment, including the entire train behind the engine, with the exception of the drive wheels, can be determined if we know the moment ΣJ_R, by the following relationship:

$$J_{SP} = \Sigma J_R \frac{t_t}{(t_t - t_n)} \qquad (47)$$

where:

t_t - the deceleration time of complete power train without engine, with traction wheels, s

t_n - the deceleration time of complete power train without engine or traction wheels, s

We begin by decelerating with all the traction wheels and record the time required to decelerate from speed v_r' to zero. We then remove two wheels, for example, and record the time required to decelerate from the same speed to zero. The moment J_{SP} is then calculated by formula (47).

Disconnecting the rear-rear axle and repeating the test, we obtain the moment of the transmission and forward-rear axle. Deducting this moment from the total moment yields the moment of the rear-rear axle. Taking now the transmission with the rear-rear axle and subtracting this value from the total, we obtain the moment of the forward-rear axle. The moment of the transmission by itself is obtained by subtracting the forward and rear values from the total.

Having the individual moments of the transmission and two rear axles, the losses owing to each component can be determined by deceleration.

1.3.2.5 Analysis of Resistive Force F_{FC} owing to Applied Torque

Given that the torque is measured behind the transmission, we have no direct way of knowing the loss in the transmission owing to the application of torque represented by the resistive force F_{FTR}. But the precise total loss behind the torquemeter is known. Thus, the energy balance equation for the case of a constant road speed can be written as equation (33) but removing the inertia ($dv_r/dt = 0$). This gives

$$F_{TDR} = F_{CMR} - \dot{F}_{BHE} - F_{FCE} = \left| \dot{F}_{RR_o} + k \cdot v_r^2 + \right.$$

$$\left. + \left[(F_{CMR} - F_{FCE} - \dot{F}_{BHE}) \left(\frac{\dot{r}_{CD} - r_{CD}^T}{\dot{r}_{CD}} \right) \right] \right| \cos\alpha_p +$$

$$+ K \cdot S_c \cdot (v_r' \cos\alpha)^2 \pm g \cdot G_T \cdot \sin\alpha_p \qquad (48)$$

To simplify matters for the purposes of this study, we can first consider $\cos\alpha_p$ as negligible (for example, if the slope is 10%, resulting in an angle α_p of 5.71°, we have a $\cos\alpha_p$ value of 0.995, which is very close to 1). We can then consider the effect of wind on the balance as cancelled since the tests were performed in both directions. In this case, $(v_r')\cos\theta$ becomes v_r^2. Lastly, the tests have shown that the difference between radii r_{CD} and r_{CD}^T is minimal on a flat road, cancelling out the additional tire rolling resistance on the ground owing to the application of torque.

Knowing the force of resistance through oil churning in both rear axles $\dot{F}_{BHE}$ ($\dot{F}_{BHE_o} + a_E \cdot v_r$), obtained previously by free-wheeling deceleration of the raised truck, the force $\dot{F}_{RR_o}$ and the k and K coefficients obtained by free-wheeling decelerations of the truck on the road, we can test at constant speed to determine the force F_{FCE} (on the same strip of road used for free-wheeling tests).

The equation becomes

$$F_{FCE} = F_{CMR} - \dot{F}_{BHE} - \dot{F}_{RR_o} - c \cdot v_r^2 \pm g \cdot G_T \cdot \sin\alpha_p \qquad (49)$$

Proceeding now to acceleration tests shifting through various transmission ratios and using different accelerator pressures, we can find a balance in which road speed and torque correspond to those of a constant test speed. Writing the energy balance equation for this point, we will obtain the above equation plus the moment of inertia of all the rotating masses. This will give

$$F_{TDR} - F_{CMR} - \dot{F}_{BHE} - F_{FCE} - \dot{F}_{RR} + \\ + c \cdot v_r^2 \pm G_T \cdot \delta_{AD} \cdot \frac{dv_r}{dt} \pm g \cdot G_T \cdot \sin\alpha_p \qquad (50)$$

This equation contains a single unknown, the δ_{AD} coefficient. Knowing this coefficient will enable us to use equation (27) to determine the η_{SP} coefficient and, from there, to use equation (22) to determine the force at the engine output, knowing the force at the wheels. The total force of drivetrain friction F_{SP} is given by

$$F_{SP} = F_{SM} - F_R \qquad (51)$$

and

$$F_{SP} - \dot{F}_{BH} = F_{FC} \qquad (52)$$

To find the force F_{FTR}, we use

$$F_{FC} - F_{FCE} = F_{FTR} \qquad (53)$$

where:

F_{FTR} - the force of rotating resistance in transmission owing to applied torque, N

In addition, efficiency η_{SP} can be determined if we know the characteristic curves for the engine (see Fig. 11). From here, knowing the fuel consumption and engine speed, we determine the engine output power N_{SM}. We then convert the torque measured at the torquemeter into power and subtract it from N_{SM}, obtaining the total transmission loss N_{TTR} (see Fig. 15). Adding N_{TTR} to the power N_{BHE} and N_{FCE} gives the total power train loss. Subtracting this total loss from N_{SM} and dividing by N_{SM} gives the efficiency η_{SP}. This explains how the ratings on Figure 17 were calculated.

1.3.3 Analysis of Combined Forces of Air and Tire Rolling Resistance (without applied torque)

These forces are represented in energy balance equation (49) by

$$F_{A+R} = \dot{F}_{RR_o} + c \cdot v_r^2 \qquad (54)$$

where:

F_{A+R} = the combined force of air and rolling resistance, N

To determine the tire rolling resistance on the ground and the air drag in the above equation, FERIC used the free-wheeling deceleration method.

Those tests were conducted on a strip of the Transport Canada test track. To take account of slight gradients, we first profiled the strip every 3 metres and determined the vertical angles. For this study, we used the right side of the federal government test track at Blainville (Québec) (see Fig. 1).

We ran free-wheeling deceleration tests on this strip of the road 15 times from A to B and 15 times from B to A, moving from about 70 km/h (≈19.5 m/s) to zero. Then from the decelerations, the energy balance equation (28) becomes:

$$0 = \underbrace{\dot{F}_{RR_o} + \dot{F}_{BH_o}}_{\dot{F}_{TR_o}} + a \cdot v_r + c \cdot v_r^2 \pm g \cdot G_T \cdot \sin\alpha_p \pm G_T \cdot \delta_A \cdot \frac{dv_r}{dt} \qquad (55)$$

where:

$\dot{F}_{TR_o}$ - the force of resistance to forward motion at near zero speed, N

c - the coefficient for rate of change of losses through combined rolling and air resistance, $N \cdot s^2/m^2$

since the force $F_{TDR} = 0$ and $k + K_F$ can be represented by a single "c" coefficient. The forces $\dot{F}_{RR_o} + \dot{F}_{BH_o}$ must be added, becoming the force $\dot{F}_{TR_o}$ (force of resistance to forward motion at near zero speed) and the force F_{FC} is eliminated in the absence of applied torque.

Equation (55) thus becomes

$$G_T \cdot \delta_A \left(\frac{dv_r}{dt} \pm \frac{g}{\delta_A} \cdot \sin\alpha_p\right) = - \dot{F}_{TR_o} - a \cdot v_r - c \cdot v_r^2 \qquad (56)$$

This relationship can be handled in one of two ways: mathematically by integration of the preceding equation or by derivation of the speed-time curve, resulting in an acceleration-time curve.

Here is how these two methods were developed.

1.3.3.1 Integration of Equation (56)

$$G_T \cdot \delta_A \left(\frac{dv_r}{dt} \pm \frac{g}{\delta_A} \cdot \sin\alpha_p\right) = - \dot{F}_{TR_o} - a \cdot v_r - c \cdot v_r^2$$

This equation is reworked as

$$G_T \cdot \delta_A \cdot \frac{dv_r}{dt} = - \dot{F}_{TR_o} - a \cdot v_r - c \cdot v_r^2 \pm G_T \cdot g \cdot \sin\alpha_p \qquad (57)$$

after which we integrate for a time from t to zero corresponding to the drop in speed from an initial speed v_r' to v_r''. This gives the equation below (see development in FERIC Technical Report TR-53):

$$t = \frac{2 \cdot \delta_A \cdot G_T}{\sqrt{4 \cdot c \cdot F_{TR_o} - a^2 \pm G_T \cdot g \cdot \sin\alpha_p}} \cdot \Bigg[$$

$$\Bigg[\operatorname{arctg} \frac{2 \cdot c \cdot v'_r + a}{\sqrt{4 \cdot c \cdot F_{TR_o} - a^2 \pm G_T \cdot g \cdot \sin\alpha_p}} -$$

$$- \operatorname{arctg} \frac{2 \cdot c \cdot v''_r + a}{\sqrt{4 \cdot c \cdot F_{TR_o} - a^2 \pm G_T \cdot g \cdot \sin\alpha_p}} \Bigg] \qquad (58)$$

This equation could be used as it stands to determine the "c" coefficient on the basis of the initial and final speeds. But a number of modifications will be made to avoid a slight error upon derivation of the distance-time relationship to obtain the speed.

Equation (58) can be written as

$$t = (m_s - n_s)/p_s \qquad (59)$$

where:

$$p_s = \left(\frac{1}{2 \cdot G_T \cdot \delta_A}\right) \cdot \sqrt{4 \cdot F_{TR_o} \cdot c - a^2 \pm G_T \cdot g \cdot \sin\alpha_p} \qquad (60)$$

$$m_s = \operatorname{arctg} \{[(1/\delta_A \cdot G_T) \cdot c \cdot v'_r + h]/B\} \qquad (61)$$

$$n_s = \operatorname{arctg} \{[(1/\delta_A \cdot G_T) \cdot c \cdot v''_r + h]/B\} \qquad (62)$$

$$h = a/2 \cdot G_T \cdot \delta_A \qquad (63)$$

Deceleration occurring from a speed v'_r to zero speed will yield

$$t_t = (n_s - o_s)/p_s \qquad (64)$$

where:

$$o_s = \text{arctg}\ (h/p_s) \tag{65}$$

The equation below can be extracted from the preceding relationships:

$$n_s = p_s\ (t_t - t) + o_s \tag{66}$$

The tangents must also be equal among themselves. Thus,

$$\tan n_s = \tan\ [p_s(t_t - t) + o_s] \tag{67}$$

Using equation (66) for n_s, introducing tan n_s and rewriting the equation gives

$$\frac{dD}{dt} = v_r = \frac{\delta_A \cdot G_T}{c} \left\{p_s \cdot \tan\ [p_s(t_t - t) + o_s] - h\right\} \tag{68}$$

By integrating the preceding equation and determining the integration constant from initial conditions t = 0 et D = 0, we obtain the distance-time relationship for moving from speed v'_r to speed v''_r:

$$D = \frac{\delta_A \cdot G_T}{c} \ln \frac{\cos\ [p_s(t_t - t) + o_s]}{\cos\ [(p_s \cdot t_t + o_s) - ht]} \tag{69}$$

Considering the total time t_t gives

$$D_t = \frac{\delta_A \cdot G_T}{c} \cdot [\ln \frac{\cos o_s}{\cos\ (p_s \cdot t_t + o_s)} - h\ t_t] \tag{70}$$

D_t - the distance corresponding to time t, m

D_{t_1} - the distance corresponding to time t_1, m

D_{t_2} - the distance corresponding to time t_2, m

D_{t_3} - the distance corresponding to time t_3, m

D_Δ - the difference in distances, m

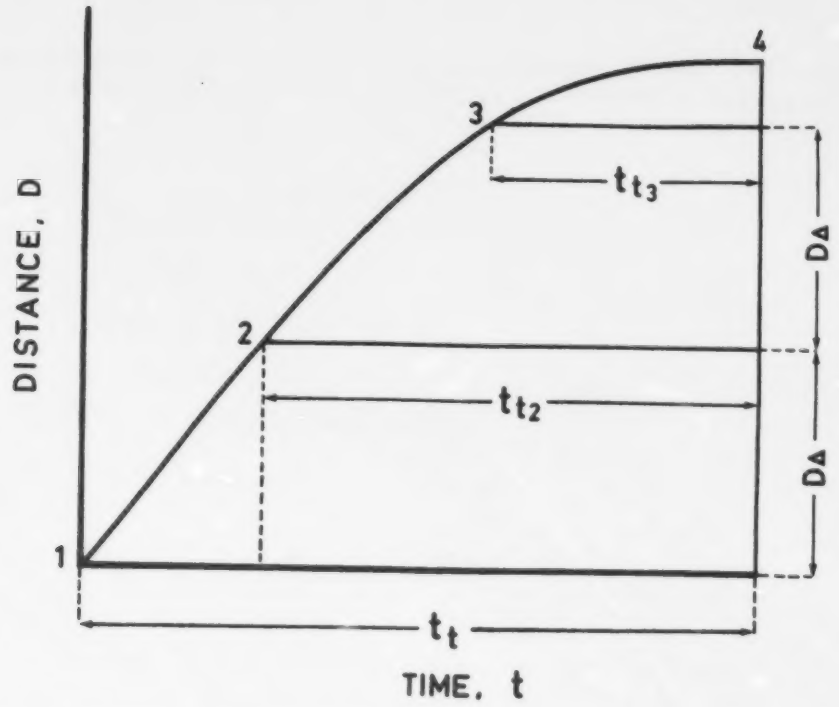

Figure 29 Diagram representing the interpretation of free-wheeling test results

Figure 29 plots a distance-time deceleration curve from point 1 to point 4. Point 3 lies very close to the maximum distance (0.9 to 0.95% of maximum distance).

Taking two total times, from point 1 to point 4 and from point 2 to point 4, and using the difference of two equations (70) will give the distance-time relationship between points 1 and 2:

$$D_\Delta = D_{t_1} - D_{t_2} = \frac{\delta_A \cdot G_T}{c} \cdot \ln \frac{\cos\ (p_s \cdot t_{t_2} + h/p_s)}{\cos\ (p_s \cdot t_{t_1} + h/p_s)} - h\ (t_{t_1} - t_{t_2}) \qquad (71)$$

The same procedure is used to obtain the distance between points 2 and 3.

$$D_\Delta = D_{t_2} - D_{t_3} = \frac{\delta_A \cdot G_T}{c} \cdot \ln \frac{\cos\ (p_s \cdot t_{t_3} + h/p_s)}{\cos\ (p_s \cdot t_{t_2} + h/p_s)} - h(t_{t_2} - t_{t_3}) \qquad (72)$$

Given that the two equations are equal to D_Δ, they can be equated by eliminating distance. In this case, we obtain a relationship with only one unknown p_s:

$$\cos^2(p_s\ t_{t_2}+h/p_s) = e^{h(t_{t_1}-2t_{t_2}+t_{t_3})} \times$$

$$\times \cos\ (p_s\ t_{t_1}+h/p_s) \times \cos\ (p_s\ t_{t_3}+h/p_s) \qquad (73)$$

p_s is found by iteration. Knowing the parameter p_s, we build the equation for the distance $2D_\Delta$ and isolate "c":

$$c = \frac{\delta_A \cdot G_T}{2D_\Delta}\left[\ln \frac{\cos\ (p_s \cdot t_{t_3}+h/p_s)}{\cos\ (p_s \cdot t_{t_1}+h/p_s)} - h\ (t_{t_1}-t_{t_3})\right] \qquad (74)$$

Knowing the "c" coefficient, we determine the initial force $\dot{F}_{TR_\circ}$ from equation (60) by isolation:

$$\dot{F}_{TR_\circ} = \frac{G_T^2 \cdot \delta^2}{c}\ (p_s^2 + h^2) \qquad (75)$$

Thus, the initial force of resistance $\dot{F}_{TR_\circ}$ and the "c" coefficient are determined without reference to road speed, which enhances the accuracy of the method.

Later on we will compare the results obtained by this method against those obtained by the above method developed by FERIC.

1.3.3.2 FERIC Method (by derivation of speed-time curve)

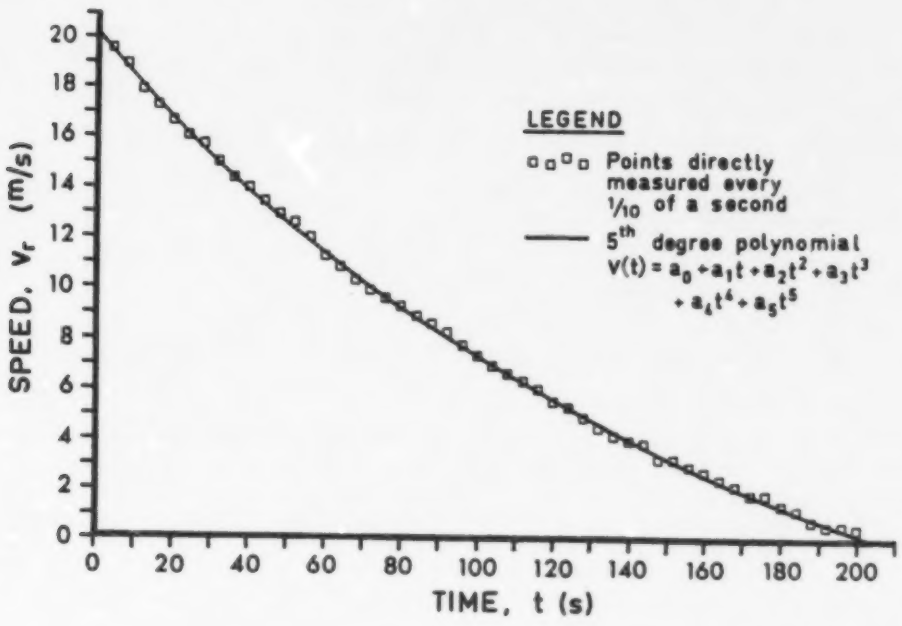
SPEED, V_r (m/s)
TIME, t (s)
LEGEND
Points directly measured every 1/10 of a second
5th degree polynomial
$V(t) = a_0 + a_1t + a_2t^2 + a_3t^3 + a_4t^4 + a_5t^5$

Figure 30 Speed-time diagram obtained by direct measurement

FERIC's instrumentation allows for simultaneous logging of distance and road speed. Making direct use of the logged speed given on Figure 30, we can find a polynomial that is an all but perfect representation of this curve, given that 2,000 recordings are made in the space of 200 seconds. Thus, the error is virtually nil. FERIC examined the polynomial degree yielding the best results. Figure 30 gives the 5th degree for the DOMEX tests.

The equation for this curve is

$$v(t) = a_0 + a_1t + a_2t^2 + a_3t^3 + a_4t^4 + a_5t^5 \qquad (76)$$

Deriving it (see Fig. 31) gives the acceleration-time equation:

$$j_{as} = a_1 + 2a_2t + 3a_3t^2 + 4a_4t^3 + 5a_5t^4$$

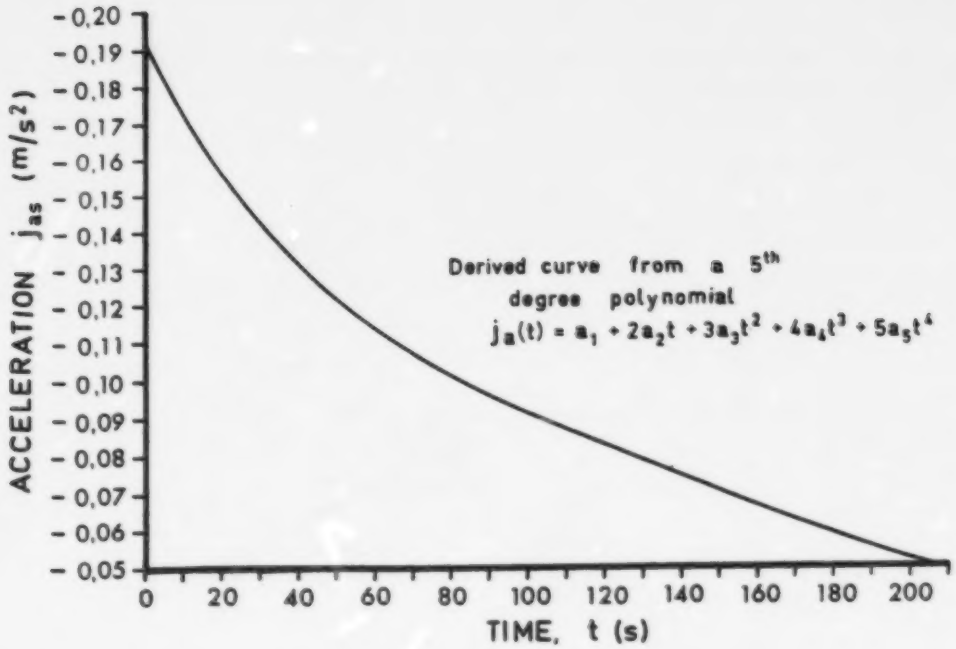

Figure 31 Diagram of translational acceleration as a function of road speed

Knowing the acceleration, we can calculate the inertia corresponding to the total force of resistance:

$$\delta_A \cdot G_T \frac{dv_r}{dt} = - \overset{\bullet}{F}_{RR_\bullet} - \overset{\bullet}{F}_{BH_\bullet} - a \cdot v_r - c \cdot v_r^2 \pm G_T \cdot g \cdot \sin\alpha_p \qquad (77)$$

The temperature of the transmission and axle oils may vary during deceleration, in which case formulae (39) and (40) can be used for continuous correction of the force $F_{BH_\bullet}$ and the "a" coefficient. Formula (77) will have the following form:

$$\delta_A \cdot G_T \frac{dv_r}{dt} + \overset{\bullet}{F}_{BH_\bullet} + a \cdot v_r \pm G_T \cdot g \cdot \sin\alpha = - \overset{\bullet}{F}_{RR_\bullet} - c \cdot v_r^2 \qquad (78)$$

This formula allows for continuous correction for gradients in the road and oil temperature variations. This unique possibility ensures the scientific accuracy of the method.

A non-linear regression was used to find the force F_{RR_o} and the "c" coefficient.

Figure 14 compares the total resistive forces obtained by the two study methods. We observe that the results are very similar, proving that the two methods are valid and comparable.

Given that FERIC makes continuous recordings of wind velocity and direction, this correction can be introduced provided that the "c" coefficient is divided into two parts, as in formula (33). Complementary tests are required for such division (see FERIC Technical Report TR-53). This will be done in the near future.

2. HEAT EXCHANGE BETWEEN ENVIRONMENT, REAR AXLES AND TRANSMISSION OF A TRUCK

In a typical heat balance for the lubricating oil relative to the environment, the temperatures in the axle housings or the transmission housing become constant. Put another way, the heat generated by churning and friction equals the heat dispelled to the outside.

Part of the heat which the oil removes from the internal walls of the power train components is used to heat the oil and the mechanical components. The remainder is dispelled to the outside.

The heat balance can be written as

$$dQ = dQ_1 + dQ_2 + dQ_3 - dQ_4 \qquad (79)$$

where:

dQ - the total friction heat generated in internal components of power train, cal

dQ_1 - the heat dispelled to exterior, cal

dQ_2 - the heat expended to raise oil temperature, cal

dQ_3 - the heat expended to raise temperature of rotating parts, cal

dQ_4 - the heat released through oil churning, cal

The heat removed by the oil from the power train components in friction for a fraction of time dt equals

$$dQ = Q_h \cdot dt \tag{80}$$

where:

Q_h - the heat received by oil during time t, cal

The differential equation for heat transmission between the oils and the environment corresponding to this same fraction of time dt is

$$dQ_1 = k' \cdot S \cdot \tau \cdot dt \tag{81}$$

where:

S - the total surface of axle housings, m^2

τ - the temperature difference between oils (in rear axle housings or transmission housing) and ambient air, °K

k' - the overall coefficient of heat transmission between oils and environment, $W/m^2 \cdot °K$

The amount of heat expended to heat the oils and power train components is given by

$$dQ_n = dQ_2 + dQ_3 = c_{tm} \cdot V \cdot d\tau + \sum_{i=1}^{i=n} G_i \cdot c_{tmi} \cdot d\tau \tag{82}$$

where:

V - the amount of oil in housings, kg

G_i - the total mass of power train components, kg

c_{tm} - the mass heat capacity of oil, $J/(kg \cdot °K)$

c_{tmi} - the mass heat capacity of power train metal i, $J/(kg \cdot °K)$

The amount of heat released through oil churning is given by

$$dQ_4 = N_{BH}^{\circ} \cdot dt \tag{83}$$

where:

N_{BH}° - the power expended to overcome oil churning resistance, W

Introducing equations (81) to (83) into equation (80) gives

$$dt = \frac{Q_n}{Q' - k \cdot S \cdot \tau} d\tau \tag{84}$$

where:

Q' - the total heat received by the oils during given fraction of time, cal; $Q' = Q + Q_4 = (1 - \eta_{SP}) \cdot N_{SM}$ = constant, given that Q rises and Q_4 drops as oil temperature rises

Q_n - the heat expended to raise temperature of oils and power train components by 1°K, cal

Researchers have shown that for oil temperatures from 20 to 90°C, we can approximate the relation between the "k" coefficient and the drop in oil temperatures in the housings (transmission) and ambient air τ, as follows:

$$k' = \frac{b \cdot k_1 \cdot \tau}{\tau_1} \tag{85}$$

where:

k_1 - the overall coefficient of heat transmission of power train components at oil temperature τ_1

b - the coefficient of proportionality

Introducing equation (85) into equation (84) and making the necessary conversions gives

$$\tau' + A_1 \cdot \tau^2 - C = 0 \tag{86}$$

where:

$$A_1 = \frac{b \cdot k_1 \cdot S}{Q_n \cdot r_1} \quad ; \quad \text{and} \quad C = \frac{Q'}{Q_n}$$

Solving this equation gives

$$r = \frac{e^{2t\sqrt{A_1 \cdot C}} - C_1}{\sqrt{\frac{A_1}{C}}\left(e^{2t\sqrt{A_1 \cdot C}} + C_1\right)} \tag{87}$$

where:

$$C_1 = C_2 \, ^{2\sqrt{A_1 \cdot C}} \tag{88}$$

at time t = o

$$C_2 = \left[\frac{1 + r_1\sqrt{\frac{A_1}{C}}}{1 - r_1\sqrt{\frac{A_1}{C}}}\right]^{\frac{1}{2\sqrt{A_1 \cdot C}}} \tag{89}$$

After introducing C_1 into equation (87) and making the necessary conversions, we obtain the equation for calculating oil temperatures for stabilization time t:

$$r_h = r_{amb} + \sqrt{\frac{C}{A_1}} \cdot \frac{\alpha - \beta \cdot e^{-2t\sqrt{A_1 \cdot C}}}{\alpha + \beta \cdot e^{-2t\sqrt{A_1 \cdot C}}} \tag{90}$$

where:

$$\alpha = \left(1 + r_1\sqrt{\frac{A_1}{C}}\right)^{\frac{1}{2\sqrt{A_1 \cdot C}}}$$

$$\beta = \left(1 - r_1\sqrt{\frac{A_1}{C}}\right)^{\frac{1}{2\sqrt{A_1 \cdot C}}}$$

For practical purposes, the most interesting temperature is the maximum operating temperature (stabilized temperature). Considering time $t \to \infty$ after the introduction of A and C gives

$$\tau_{mu} - \tau_{amb} + \sqrt{\frac{Q' \cdot \tau_1}{b \cdot k_1 \cdot S}} \qquad (91)$$

We see from equation (91) that the maximum operating temperature (stabilization temperature) depends upon heat Q' received by the oil from the product of $k_1 \cdot S$ and the ambient temperature.

Knowing temperatures τ_{mu} and τ_{amb}, the amount of heat Q' and the surface S, formula (91) can be used to derive the coefficient $b \cdot k \sqrt{\tau_1}$. Introducing this in the formula for A and knowing heat Q' and Q_n, we can use formula (90) to calculate the oil temperatures upon stabilization on the road. Formula (91) shows that the oil temperatures upon stabilization are directly dependent upon the ambient temperature. In other words, if we know the oil temperature for one ambient temperature, we can simply add or subtract to obtain the oil temperature for the other ambient temperature.

3. PROPERTIES OF TEST OILS

3.1 Engine Oils

Reference	15W40	at	40°C	→	100.7 cSt
		at	100°C	→	13.5 cSt
Synthetic	5W30	at	38°C	→	83.3 cSt
		at	98°C	→	10.33 cSt

3.2 Power Train Oils

Reference	80W90	at	40°C	→	158 cSt
		at	100°C	→	16.7 cSt
Synthetic	75W90	at	40°C	→	100 cSt
		at	100°C	→	15.8 cSt

DEFINITION OF SYMBOLS

a - Coefficient for rate of change of oil churning losses in transmission and two rear axles, N·s/m

a_E - Coefficient for rate of change of oil churning losses in two rear axles, N·s/m

a_m - Wheel acceleration, m/s^2

b - Coefficient of proportionality

c - Coefficient for rate of change of losses through combined rolling and air resistance, $N \cdot s^2/m^2$

c_{tm} - Mass heat capacity of oil J/(kg·°K)

c_{tmi} - Mass heat capacity of power train metal i, J/(kg·°K)

D - Distance, m

D_t - Distance corresponding to time t, m

D_{t_1} - Distance corresponding to time t_1, m

D_{t_2} - Distance corresponding to time t_2, m

D_{t_3} - Distance corresponding to time t_3, m

D_Δ - Difference in distances, m

dQ - Total friction heat generated in internal components of power train, cal

dQ_1 - Heat dispelled to exterior, cal

dQ_2 - Heat expended to raise oil temperature, cal

dQ_3 - Heat expended to raise temperature of rotating parts, cal

dQ_4 - Heat released through oil churning, cal

F_{A+R} - Combined force of air and rolling resistance, N

F°_{BH} - Total force of resistance to churning without applied torque, N. Comprised of initial force of churning resistance (upon starting) and of an effort varying linearly with road speed.

$F^{\circ}_{BH_{\bullet}}$ - Initial force of resistance to churning where superscript "°" designates zero torque and subscript "•" designates near zero speed, N

F°_{BHE} - Force of resistance through oil churning in two rear axles, N

$F^{\circ}_{BHE_{\bullet}}$ - Force of resistance at near zero speed through oil churning in two rear axles, N

F_C - Force of rolling resistance owing to camber of forward (drive) wheels, N

F_{CMR} - Tangential force obtained by torquemeter measurement and corrected for the wheels, N

F_{DRR} - Dynamic force of tire rolling resistance (including all rolling resistance factors identified in FERIC Technical Report TR-55, D.9.1), N

F_{FC} - Force of resistance owing to power train friction with applied drive torque, N

F_{FCE} - Total force of rotating resistance in two rear axles owing to applied torque (friction), N

F_{FTR} - Force of rotating resistance in transmission owing to applied torque, N

$F^{\circ}_{TR_{\circ}}$ - Force of resistance to forward motion at near zero speed, N

F_{I} - Force of vehicle inertia (acceleration or deceleration), N

F_{INC} - Directional force of resistance owing to vertical gradient in road, N. It equals $g \cdot G_T \cdot \sin\alpha_D$ where G_T is total vehicle mass in kg, α_D is angle of road incline and g is gravitational acceleration

F_{IR} - Force of wheel and drivetrain inertia, N

F_{IRM} - Force of resistance through engine inertia, N

F_{M} - Additional force owing to application of torque at drive wheels, N

F_{RA} - Dynamic force of air resistance (including effect of wind), N

F°_{RR} - Force of rolling resistance on ideally flat, straight road without applied torque (traction), N. Superscript "°" designates zero traction torque

$F^{\circ}_{RR_{\circ}}$ - Force of rolling resistance at near zero speed, N

F_{SC} - Force of rolling resistance owing to suspension type and vibration, N

F_{SD} - Force of rolling resistance owing to ground deformation, N

F_{SMD} - Dynamic drive force at engine output, N

F_{SP} - Dynamic force of power train resistance, N

F_{TDR} - Total dynamic traction at traction wheels (including force of inertia upon acceleration or deceleration), N

$F^{\circ}_{TR_{\circ}}$ - Force of resistance to forward motion at near zero speed, N

F_{δ} - Force of rolling resistance owing to angle of side slip of front (drive) wheels, N and appears at the moment the truck negotiates a curve

G_i - Total mass of power train components, kg

G_R - Mass of wheel with tire, kg

G_T - Total vehicle mass, kg

g - Gravitational acceleration, m/s^2

i_{EA} - Rear axle ratio

i_{TR} - Transmission ratio

J - Combined moments of inertia of traction wheels and power train, $kg \cdot m^2$

J_M - Engine moment of inertia, $kg \cdot m^2$

J_R - Moment of inertia of a tire with its rim, $kg \cdot m^2$

J_{SP} - Power train moment of inertia, $kg \cdot m^2$

j_{as} - dv_r/dt - vehicle translational acceleration, m/s^2

K - Coefficient for rate of change of air drag losses as a function of squared speed, $N \cdot s^2/m^4$

k - Coefficient for rate of change of rolling resistance losses as a function of squared speed, $N \cdot s^2/m^2$

k' - Overall coefficient of heat transmission between oils and environment, $W/m^2 \cdot °K$

k_1 - Overall coefficient of heat transmission of power train components at oil temperature τ_1

M_{CM} - Torque measured at torquemeter, $N \cdot m$

M_M - Dynamic engine rotating moment under variable operating conditions, $N \cdot m$

M_{PT} - Moment corresponding to total transmission losses (through oil churning and friction), $N \cdot m$

N_{A+R} - Power absorbed by tire rolling and air resistance, hp

$\dot{N}_{BH}$ - Power expended to overcome oil churning resistance, W

$\dot{N}_{BHE}$ - Power absorbed in two rear axles through oil churning, hp

$\dot{N}_{BHT}$ - Power absorbed by churning of transmission oil, hp

N_{FCE} - Power absorbed in two rear axles by friction with applied torque, hp

N_{FCT} - Power absorbed by friction in transmission with applied torque, hp

N_R - Power at drive wheels, kW

N_{SM} - Engine output power (engine mounted in truck), kW

N_{TC} - Total power obtained by measured fuel consumption, hp

N_{TTR} - Total power absorbed in transmission, hp

Q' - Total heat received by oils during given fraction of time, cal; $Q' = Q + Q_4 = (1 - \eta_{SP}) \cdot N_{SM}$ = constant, given that Q rises and Q_4 drops as oil temperature rises

Q_h - Heat received by oil during time t, cal

Q_n - Heat expended to raise temperature of oils and power train components by 1°K, cal

r_{CD}^{T} - Radius of loaded traction tires with torque applied, m

r_{CD}° - Radius of loaded traction tires without applied torque, m

r_1 - Free tire radius, m

S - Total surface of axle housings, m^2

S_C - Corrected vehicle frontal area, m^2

t - Deceleration time from speed v_r' to speed v_r'', s

t_n - Deceleration time of complete power train without engine or traction wheels, s

t_s - Time to travel distance D, s

t_t - Deceleration time of complete power train without engine, with traction wheels, s

V - Amount of oil in housings, kg

v_r - Road speed, m/s

v'_r - Initial road speed, m/s

v''_r - Intermediate deceleration speed, m/s

v^v_r - Road speed corrected for wind velocity, m/s

α_p - Angle of road decline, degrees

δ_A - Coefficient for vehicle rotating masses

δ_{AD} - Dynamic coefficient for calculating all rotating and translational masses, including engine

η_B - Coefficient for oil churning in various components

η°_{BH} - Efficiency with no torque applied

η_F - Coefficient for internal friction between gears

η_{FC} - Coefficient for friction as a function of road (rotating) speed and transmitted torque

η_{JE} - Coefficient for friction in sealing joints

η_{PO} - Coefficient for oil pump efficiency (if applicable)

η_{ROU} - Coefficient for friction in bearings

η_{SP} - Overall power train efficiency

θ - Angle of wind direction relative to vehicle longitudinal axis, degree

$\sum_{R}^{n} J$ - Total moment of traction wheels, $kg \cdot m^2$

τ - Temperature difference between oils (in rear axle housings or transmission housing) and ambient air, °K

REFERENCES

Avtomobilnii transport i dorogi, Minsk, visheishaia shkola, 1976.

FULLER, Dudley D., Theory and practice of lubrication for engineers, second edition, John Wiley and Sons, Inc. 1984.

KLAMANN, Dieter, Lubricants and related products, Verlag Chemie GrubH, D-6940 Weinheim, 1984.

LJUBIC, D.A., Analysis of productivity and cost of forestry transportation. PART ONE: Pilot study to determine the factors for analysis of commercial vehicle power consumption and road performance, Forest Engineering Research Institute of Canada, Tech. Rep. n° TR-53, June 1982, 49 p.

LJUBIC, D.A., Analysis of productivity and cost of forestry transportation. PART TWO: Theoretical analysis of the impact of vehicle operating conditions on power losses and experimental determination of the resistance forces attributable to oil churning, Forest Engineering Research Institute of Canada, Tech. Rep. n° TR-55, April 1984, 80 p.

LJUBIC, D.A., Analysis of productivity and cost of forestry transportation. PART THREE: Theoretical analysis of the impact of vehicle operating conditions of power losses, experimental determination of rolling and air resistance forces, Forest Engineering Research Institute of Canada, Tech. Rep. n° TR-61, November 1985, 74 p.

PETROUSHOV, V.A., MOSKOVKIN, V.V., EVGRAFOV, A.N., Moschtnostnoi Balans automobilila, Mashinostroenie, Moskva 1984.